

Self-Consistent Conformal Prediction

Lars van der Laan^{*,1} and Ahmed M. Alaa²

¹Department of Statistics, University of Washington, USA

²Department of Computational Precision Health, UC Berkeley and UCSF, USA

*Corresponding author: lvdlaan@uw.edu

April 23, 2024

Abstract

In decision-making guided by machine learning, decision-makers may take identical actions in contexts with identical predicted outcomes. Conformal prediction helps decision-makers quantify uncertainty in point predictions of outcomes, allowing for better risk management for actions. Motivated by this perspective, we introduce *Self-Consistent Conformal Prediction* for regression, which combines two post-hoc approaches — Venn-Abers calibration and conformal prediction — to provide calibrated point predictions and compatible prediction intervals that are valid conditional on model predictions. Our procedure can be applied post-hoc to any black-box model to provide predictions and inferences with finite-sample prediction-conditional guarantees. Numerical experiments show our approach strikes a balance between interval efficiency and conditional validity.

Keywords— Distribution-free, uncertainty quantification, conformal prediction, conditional predictive inference, Venn-Abers calibration, isotonic calibration

1 Introduction

Incorporating machine learning into decision-making processes has shown significant promise in improving post-decision outcomes, such as better medical treatments and reduced costs (Kang et al., 2015; Bhardwaj et al., 2017; Marr, 2019). Particularly in safety-critical sectors, such as healthcare, it is important to ensure decisions inferred from predictions made by machine learning models are reliable, under minimal assumptions

(Mandinach et al., 2006; Veale et al., 2018; Char et al., 2018; Quest et al., 2018; Vazquez and Facelli, 2022). As a response, there has been growing interest in predictive inference approaches to decision-making, allowing for rigorous risk assessment by quantifying deviations of outcomes from model predictions via prediction intervals (Patel, 1989; Heskes, 1996).

Conformal prediction (CP) is a popular, model-agnostic, and distribution-free framework for predictive inference, which can be applied post-hoc to any prediction pipeline (Vovk et al., 2005; Shafer and Vovk, 2008; Balasubramanian et al., 2014; Lei et al., 2018). Given a prediction issued by a black-box model, CP outputs a prediction interval that is guaranteed to contain the unobserved outcome with a user-specified probability (Lei et al., 2018). However, a limitation of CP is that this prediction interval only provides valid coverage marginally, when averaged across all possible contexts – with ‘context’ referring to the information available for decision-making. Constructing informative prediction intervals that offer context-conditional coverage is generally unattainable without making additional distributional assumptions (Vovk, 2012; Lei and Wasserman, 2014; Barber et al., 2021). Consequently, there has been an upsurge in research developing CP methods that offer weaker, yet practically useful, notions of conditional validity (Johansson et al., 2014, 2018; Tibshirani et al., 2019; Boström and Johansson, 2020; Romano et al., 2020; Sesia and Romano, 2021; Boström et al., 2021; Jung et al., 2022; Bastani et al., 2022; Deng et al., 2023; Guan, 2023; Hore and Barber, 2023; Gibbs et al., 2023; Ding et al., 2023; Jin and Ren, 2024).

Contributions. To avoid the curse of dimensionality inherent in context-specific validity, we introduce a self-consistency objective that aims to construct prediction intervals with model prediction-conditional coverage guarantees. We then propose Self-Consistent Conformal Prediction (SC-CP), which combines two post-hoc approaches — Venn-Abers calibration (Vovk and Petej, 2012) and split CP (Lei et al., 2018) — to simultaneously provide a Venn-Abers set of calibrated point predictions and compatible conformal prediction intervals that, in finite samples, are valid conditionally on calibrated model predictions.

2 Problem setup

2.1 Notation

We consider a standard regression setup in which the input $X \in \mathcal{X} \subset \mathbb{R}^d$ corresponds to contextual information available for decision-making, and the output $Y \in \mathcal{Y} \subset \mathbb{R}$ is an outcome of interest. We assume that we have access to a calibration dataset $\mathcal{C}_n = \{(X_i, Y_i)\}_{i=1}^n$ comprising n *i.i.d.* data points drawn from an unknown distribution $P := P_X P_{Y|X}$. We assume access to a black-box predictor $f : \mathcal{X} \mapsto \mathcal{Y}$, obtained by training an ML model on a dataset that is independent of \mathcal{C}_n . Throughout this paper, we do not make any assumptions on the model f or the distribution P .

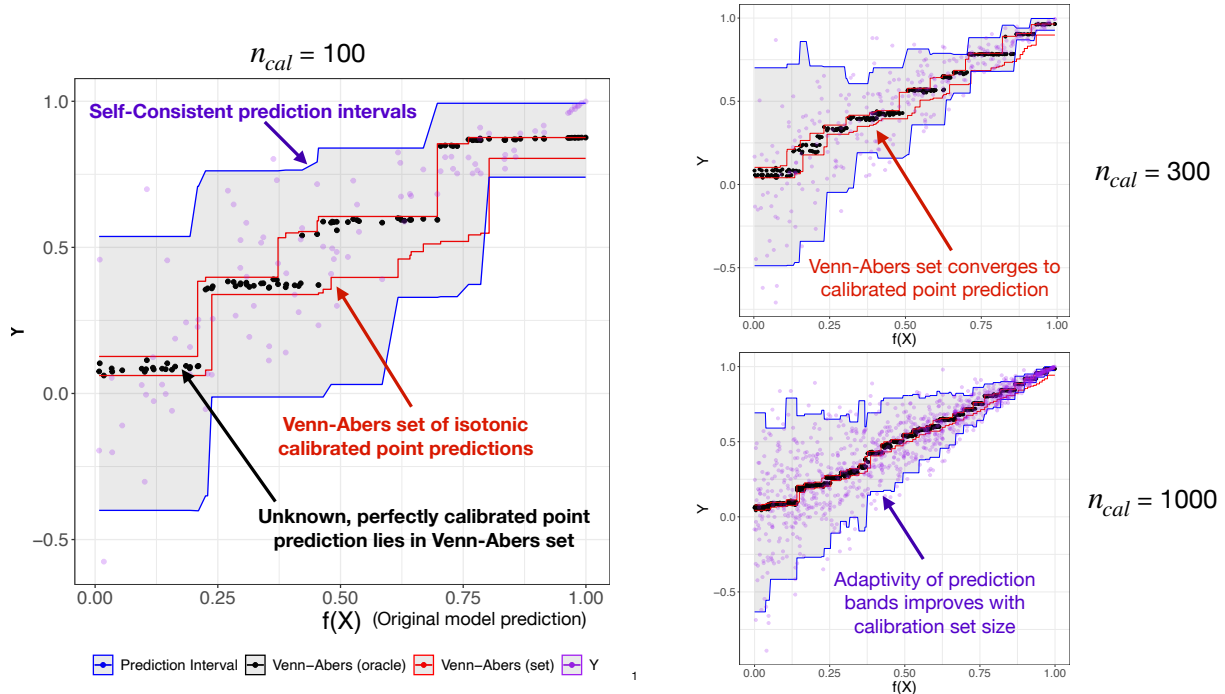


Figure 1: Illustration of Venn-Abers set predictions and conformal prediction intervals output by Self-Consistent Conformal Prediction. x-axis displays original, pre-calibration model predictions.

2.2 Conditional predictive inference and challenges

Let (X_{n+1}, Y_{n+1}) be a new data point drawn from P independently of the calibration data \mathcal{C}_n . **Our high-level aim** is to develop a *predictive inference* algorithm that constructs a prediction interval $\hat{C}_n(X_{n+1})$ around the point prediction issued by the black-box model, i.e., $f(X_{n+1})$. For this prediction interval to be deemed *valid*, it should *cover* the true outcome Y_{n+1} with a probability $1 - \alpha$. Conformal prediction (CP) is a method for predictive inference that can be applied in a post-hoc fashion to any black-box model (Vovk et al., 2005). The vanilla CP procedure issues prediction intervals that satisfy the marginal coverage condition:

$$\mathbb{P}(Y_{n+1} \in \hat{C}_n(X_{n+1})) \geq 1 - \alpha, \quad (1)$$

where the probability \mathbb{P} is taken with respect to the randomness in \mathcal{C}_n and (X_{n+1}, Y_{n+1}) . However, marginal coverage might lack utility in decision-making scenarios where decisions are context-dependent. A prediction band $\hat{C}_n(x)$ achieving 95% coverage may exhibit arbitrarily poor coverage for specific contexts x , or achieve coverage on predictions that are already less uncertain or less relevant to the decision-maker. Ideally, we would like this coverage condition to hold for each context $x \in \mathcal{X}$, i.e., the conventional notion of “conditional

validity” requires

$$\mathbb{P}(Y_{n+1} \in \widehat{C}_n(X_{n+1}) | X_{n+1} = x) \geq 1 - \alpha, \quad (2)$$

for all $x \in \mathcal{X}$. However, previous work has shown that it is impossible to achieve (2) without distributional assumptions (Vovk, 2012; Lei and Wasserman, 2014; Barber et al., 2021).

Relaxing context-conditional coverage. While context-conditional validity as in (2) is generally unachievable without distributional assumptions, it is feasible to attain weaker forms of conditional validity. Given any finite set of groups \mathcal{G} and a grouping function $G : \mathcal{X} \times \mathcal{Y} \rightarrow \mathcal{G}$, Mondrian-CP offers coverage conditional on group membership, that is, $\mathbb{P}(Y_{n+1} \in \widehat{C}_n(X_{n+1}) | G(X_{n+1}, Y_{n+1}) = g) \geq 1 - \alpha, \forall g \in \mathcal{G}$ (Vovk et al., 2005; Romano et al., 2020; Boström et al., 2021). Multivald-CP improves upon Mondrian-CP by also providing coverage conditional on a threshold value that defines the prediction interval (Jung et al., 2022; Bastani et al., 2022; Noarov et al., 2023). Expanding upon group- and context-conditional coverage, Deng et al. 2023 introduced a *multicalibration* objective that seeks to satisfy, for all f in an (infinite-dimensional) class \mathcal{F} of covariate shifts (i.e., weightings), the property:

$$\mathbb{E}[f(X_{n+1})\{(1 - \alpha) - 1\{Y_{n+1} \in \widehat{C}_n(X_{n+1})\}\}] = 0. \quad (3)$$

A curse of dimensionality. Gibbs et al. 2023 proposed a regularized CP framework for (approximately) achieving (3) that provides a means to trade off the efficiency (i.e., width) of prediction intervals and the degree of conditional coverage achieved, interpolating between marginal and conditional guarantees. However, Barber et al. 2021 and Gibbs et al. 2023 demonstrate the existence of a “curse of dimensionality”: as the dimension of the context increases, smaller classes of covariate shifts must be considered to retain the same level of efficiency. For group-conditional coverage, this curse of dimensionality manifests in the size of the subgroup class \mathcal{G} (Barber et al., 2021) via its VC dimension (Vapnik et al., 1994). Thus, especially in data-rich contexts, prediction intervals with meaningful multicalibration guarantees may be too wide for decision-making.

2.3 A dual calibration objective

In this section, we propose a practical notion of conditional validity that is feasible in finite samples and avoids the curse of dimensionality inherent in context-conditional multicalibration. This notion is motivated by the observation that the model prediction $f(x)$ can be viewed as a scalar dimension reduction of the context x that is designed to be predictive of the outcome. Consequently, given access to the model $f(\cdot)$, a natural relaxation of the context-conditional validity objective in (2) is prediction-conditional validity,

i.e., $P(Y_{n+1} \in \widehat{C}_n(X_{n+1}) | f(X_{n+1})) \geq 1 - \alpha$. Prediction-conditional validity is particularly useful when the prediction interval is used to quantify the deviation of the predicted outcome $f(X_{n+1})$ from the true outcome Y_{n+1} , as it ensures that the interval width adapts to the output of the model $f(\cdot)$. Given the central role of point predictions in this objective and decision-making more broadly, it is important that the model $f(\cdot)$ is well-calibrated to ensure its outputs are reliable and accurately reflect actual outcomes.

Self-consistency. In this work, we address the dual objective of providing calibrated point predictions and compatible prediction intervals that satisfy the following desiderata:

- (i) **Self-Consistent Point Predictions:** $f(X_{n+1}) = \mathbb{E}[Y_{n+1} | f(X_{n+1})]$.
- (ii) **Self-Consistent Prediction Intervals:** $\mathbb{P}(Y_{n+1} \in \widehat{C}_n(X_{n+1}) | f(X_{n+1})) \geq 1 - \alpha$.

Formally, for two random vectors \mathbf{X} and \mathbf{Y} , we say that \mathbf{Y} is self-consistent for \mathbf{X} if $E[\mathbf{X}|\mathbf{Y}] = \mathbf{Y}$ almost surely (Definition 2.1 in [Flury and Tarpey 1996](#)). The concept of self-consistency traces back to Efron, who introduced it in 1967 to characterize estimators for a distribution function in the context of censored data ([Efron, 1967](#)). Desideratum (i) states that the (black-box) prediction $f(X_{n+1})$ should be self-consistent for the true outcome Y_{n+1} — a condition also known as “perfect calibration” ([Gupta et al., 2020](#); [van der Laan et al., 2023](#)). There is extensive literature on how the calibration of point predictions issued by machine learning models aids in their reliability, trustworthiness, and interpretation ([Zadrozny and Elkan, 2001](#); [Bella et al., 2010](#); [Guo et al., 2017](#); [Davis et al., 2017](#)). Desideratum (ii) presents a relaxation of the infeasible coverage condition in (2), requiring the prediction interval for X_{n+1} to provide valid coverage for Y_{n+1} within contexts with identical (self-consistent) outcome predictions. Desideratum (i) also ensures the prediction interval $\widehat{C}_n(X_{n+1})$ is centered around a conditionally unbiased prediction, meaning the interval’s width is driven by variation in the outcome rather than by bias in the prediction.

Uncertainties in decision-making. Desiderata (i) and (ii) can also be motivated from a decision-making scenario where point predictions are used to determine actions and prediction intervals are used to selectively apply these actions. Consider a decision-making process guided by the black-box model $f(\cdot)$ where identical actions $a(f(x)) \in \mathcal{A}$ are prompted for contexts $x \in \mathcal{X}$ sharing the same predicted value $f(x)$. For example, if $f(\cdot)$ predicts the future biomarker (e.g., patient antibiotic resistance) value in a medical setting, a clinician may apply an intervention (e.g., an antibiotic) for patient x based on the value of $f(x)$ ([Feretzkis et al., 2021](#); [Sakagianni et al., 2023](#)). The width of the prediction interval, $\widehat{C}_n(x)$, serves as an additional signal for decision-making. In the set of patients with the same point prediction $\{x' \in \mathcal{X} : \forall f(x') = \bar{f}\}$, the intervention may be applied selectively, focusing on contexts where the interval width $\widehat{C}_n(\cdot)$ is sufficiently small in order to minimize the risk of over- or under-treatment and unnecessary side effects. Desideratum (i) implies that point predictions from $f(\cdot)$ are accurate, on average, for all contexts assigned the same action.

For instance, for all patients treated with an antibiotic, the average antibiotic resistance for this group should indeed be low. Desideratum (ii) implies that prediction intervals are valid within the subset of all contexts receiving the same action. For example, within the set of patients treated with an antibiotic, the intervals should accurately cover their true antibiotic resistance ranges.

3 Self-Consistent Conformal Prediction

A key advantage of CP is that it can be applied post-hoc to any black-box model f without disrupting its point predictions. However, desideratum (i) introduces a self-consistency requirement for the point predictions of f , thereby interfering with the underlying model specification. In this section, we introduce a modified version of CP, Self-Consistent CP (SC-CP), that satisfies a form of (i) and (ii) while preserving all the favorable properties of CP, including its finite-sample validity and post-hoc applicability.

Our predictive inference procedure combines **two post-hoc** approaches: Venn-Abers calibration (Vovk and Petej, 2012) and split CP (Lei et al., 2018). The key idea behind our method is to first apply a post-hoc calibration step to the point predictions using isotonic regression to determine a self-consistent point prediction satisfying (i). Next, we apply a prediction-conditional form of CP to the calibration step (Lei et al., 2018) to achieve the coverage guarantee in (ii). Before describing our complete procedure in Section 3.3, we provide background on isotonic calibration and introduce Venn-Abers calibration for regression.

3.1 Preliminaries on point calibration

Following the framing of van der Laan et al. 2023 (see also Gupta et al. 2020), a *point calibrator* is a post-hoc procedure that aims to learn a transformation $\theta_n : \mathbb{R} \rightarrow \mathbb{R}$ of the black-box model f such that: (1) $\theta_n(f(X_{n+1}))$ is (approximately) self-consistent for Y_{n+1} ; and (2) $\theta_n \circ f$ is comparably predictive to f . Condition (2) ensures that in the process of achieving (1), the quality of the model f is not compromised, and excludes trivial calibrators such as $\theta_n(f(\cdot)) := \frac{1}{n} \sum_{i=1}^n Y_i$ (Gupta and Ramdas, 2021).

Commonly-employed point calibrators include Platt’s scaling (Platt et al., 1999), histogram (or quantile) binning (Zadrozny and Elkan, 2001), and isotonic calibration (Zadrozny and Elkan, 2002; Niculescu-Mizil and Caruana, 2005). Mechanistically, these point calibrators learn θ_n by regressing the outcomes $\{Y_i\}_{i=1}^n$ on the model predictions $\{f(X_i)\}_{i=1}^n$. Importantly, however, point calibration fundamentally differs from the regression task of learning $\mathbb{E}[Y|f(X)]$, as calibration can be achieved without smoothness assumptions, allowing for misspecification of the regression task (Gupta et al., 2020). Histogram binning is a simple and distribution-free calibration procedure (Gupta et al., 2020; Gupta and Ramdas, 2021) that learns θ_n via a histogram regression over a finite (outcome-agnostic) binning of the output space $f(\mathcal{X})$. Isotonic calibration

is an outcome-adaptive binning method that uses isotonic regression (Barlow and Brunk, 1972) to learn θ_n by minimizing the empirical mean square error over all 1D piece-wise constant, monotone nondecreasing transformations. Isotonic calibration is distribution-free — it does not rely on monotonicity assumptions — and, in contrast with histogram binning, it is tuning parameter-free and naturally preserves the mean-square error of the original predictor (as the identity transform is monotonic) (van der Laan et al., 2023). A key limitation of histogram binning and isotonic calibration is that their self-consistency guarantees are only approximate, and desideratum (i) only holds asymptotically.

3.2 Venn-Abers calibration

In this section, we propose Venn-Abers calibration for regression, which provides finite-sample self-consistency guarantees and extends the original Venn-Abers procedure for binary classification (Vovk and Petej, 2012).

Oracle procedure. To motivate Venn-Abers calibration, we begin by providing an *oracle* variant of isotonic calibration that provides a self-consistent point prediction *in finite samples*. To this end, we define an *isotonic calibrator class* Θ_{iso} to consist of all univariate, piecewise constant functions that are monotonically nondecreasing with at most $k(n)$ constant segments, with $k(n) \in \mathbb{N} \cup \{\infty\}$ user-specified. Let $\mathcal{C}_{n+1}^* = \{(X_i, Y_i)\}_{i=1}^{n+1}$ be an oracle-augmented calibration set obtained by combining observed data $\mathcal{C}_n \cup \{X_{n+1}\}$ with the unobserved outcome Y_{n+1} . Given the initial black-box model f , calibration data \mathcal{C}_{n+1}^* , and an isotonic calibrator class Θ_{iso} , an oracle Venn-Abers prediction is given by $f_{n+1}^*(X_{n+1}) := \theta_{n+1}(f(X_{n+1}))$ where θ_{n+1} is obtained via isotonic calibration of f by solving:

$$\theta_{n+1} \in \operatorname{argmin}_{\theta \in \Theta_{\text{iso}}} \sum_{i=1}^{n+1} \{Y_i - \theta(f(X_i))\}^2.$$

Here, we follow Groeneboom and Lopuhaa (1993) in taking θ_{n+1} to be the unique càdlàg piece-wise constant solution that can only take jumps at observed values of the predictions. Using the first-order conditions characterizing the optimizer θ_{n+1} and exchangeability, we can show that this oracle prediction is self-consistent for Y_{n+1} (desideratum (i)), i.e., $f_{n+1}^*(X_{n+1}) = \mathbb{E}[Y_{n+1} | f_{n+1}^*(X_{n+1})]$.

Practical procedure. The (practical) Venn-Abers calibration procedure is outlined in Algorithm 1. Since the outcome Y_{n+1} is unknown in the oracle procedure, the Venn-Abers calibration algorithm instead iterates over imputed outcomes $y \in \mathcal{Y}$ for Y_{n+1} and applies isotonic calibration to the augmented dataset $\mathcal{C}_n \cup \{(X_{n+1}, y)\}$ to produce a set of point predictions $\{f_n^{(X_{n+1}, y)}(X_{n+1}) : y \in \mathcal{Y}\}$. By design, this set prediction is guaranteed *in finite samples* to include a self-consistent point prediction, namely, the oracle Venn-Abers prediction $f_{n+1}^*(X_{n+1}) = f_n^{(X_{n+1}, Y_{n+1})}(X_{n+1})$. In small samples, standard isotonic calibration may overfit, leading to poor finite-sample calibration. Venn-Abers calibration accounts for overfitting by widening the

Algorithm 1 Venn-Abers Calibration for Regression

Input: Calibration data $\mathcal{C}_n = \{(X_1, Y_1), \dots, (X_n, Y_n)\}$, isotonic calibrator class Θ_{iso} , black-box model f , context $x \in \mathcal{X}$.

- 1: **for** each $y \in \mathcal{Y}$ **do**
- 2: Set augmented dataset $\mathcal{C}_n^{(x,y)} := \mathcal{C}_n \cup \{(x, y)\}$;
- 3: Apply isotonic calibration to f using $\mathcal{C}_n^{(x,y)}$ and Θ_{iso} :
 $\theta_n^{(x,y)} := \operatorname{argmin}_{\theta \in \Theta_{\text{iso}}} \sum_{i \in \mathcal{C}_n^{(x,y)}} \{Y_i - \theta \circ f(X_i)\}^2$.
 $f_n^{(x,y)} := \theta_n^{(x,y)} \circ f$.
- 4: **end for**

Output: Venn-Abers prediction $\{f_n^{(x,y)}(x) : y \in \mathcal{Y}\}$.

set prediction in such scenarios, thus indicating greater uncertainty in the value of the self-consistent point prediction (Johansson et al., 2023). Unlike prediction intervals, the stability of isotonic regression implies that the Venn-Abers set prediction converges to a self-consistent point prediction as the calibration set size grows (Caponnetto and Rakhlin, 2006; Vovk and Petej, 2012), and each point prediction in the set enjoys the same large-sample self-consistency guarantees for isotonic calibration (van der Laan et al., 2023).

Computational considerations. When the outcome space \mathcal{Y} is non-discrete, Alg. 1 may be infeasible to compute exactly, and in such cases, it can be approximated by discretizing \mathcal{Y} . However, even in the non-discrete case, the range of the Venn-Abers set prediction can be feasibly computed as $[f_n^{(x,y_{\min})}(x), f_n^{(x,y_{\max})}(x)]$, with $[y_{\min}, y_{\max}] := \operatorname{range}(\mathcal{Y})$, in light of the min-max representation of the isotonic regression solution (Lee, 1983). The primary computational cost of Alg. 2 lies in the isotonic calibration step, which needs to be executed for each data point for which a prediction is desired. However, isotonic regression (Barlow and Brunk, 1972) can be efficiently and scalably computed (in linear time) using standard software for univariate regression trees with monotonicity constraints, such as the implementations in R and Python of `xgboost` (Chen and Guestrin, 2016). For large-scale data, computational time can be further reduced by limiting the maximum number of constant segments, $k(n)$, for elements in Θ_{iso} . This constraint can be enforced in `xgboost` through the arguments for maximum tree depth and minimum leaf node size. Algorithm 1. must be applied separately for every context $x \in \mathcal{X}$ for which a calibrated prediction is desired. However, Algorithm 1 only depends on the contexts $\{X_i\}_{i=1}^n \cup \{x\}$ through the model predictions $\{f(X_i)\}_{i=1}^n \cup \{f(x)\}$. As a result, to reduce computational complexity, it is possible to approximate Algorithm 1 by discretizing the context space \mathcal{X} by taking the preimage of a discretization of the prediction space $f(\mathcal{X}) = \{f(x) : x \in \mathcal{X}\} \subset \mathbb{R}$. For example, in our experiments, we used \mathcal{C}_n and quantile binning to discretize $f(\mathcal{X})$ into 200 equal-frequency bins.

3.3 SC-CP by Conformalizing Venn-Abers Predictors

In this section, we propose self-consistent conformal prediction, which conformalizes the Venn-Abers calibration procedure to provide prediction intervals centered around the Venn-Abers set prediction that are self-consistent in the sense of desideratum (ii).

Oracle procedure. To motivate SC-CP, we begin by providing an oracle procedure to achieve desideratum (ii). Let $f_{n+1}^*(X_{n+1}) = f_n^{(X_{n+1}, Y_{n+1})}(X_{n+1})$ be the oracle Venn-Abers prediction obtained by isotonic calibrating f using the oracle-augmented calibration dataset $\mathcal{C}_{n+1}^* = \{(X_i, Y_i)\}_{i=1}^{n+1}$. Next, let $S_i := |Y_i - f_{n+1}^*(X_i)|$ for $i \in [n+1]$ be the conformity scores. For a quantile level $\alpha \in (0, 1)$, we define the ‘‘pinball’’ quantile loss function ℓ_α as

$$\ell_\alpha(y, f(x)) := \begin{cases} \alpha(y - f(x)), & \text{if } y \geq f(x), \\ (1 - \alpha)(f(x) - y) & \text{if } y < f(x). \end{cases}$$

Our SC-CP interval is then given by the interval $C_{n+1}^*(X_{n+1}) := f_{n+1}^*(X_{n+1}) \pm \rho_{n+1}^*(X_{n+1})$, where ρ_{n+1}^* is an estimate of the $1 - \alpha$ prediction-conditional quantile of S_{n+1} , computed via quantile regression as:

$$\rho_{n+1}^* \in \underset{\theta \circ f_{n+1}^*; \theta: \mathbb{R} \rightarrow \mathbb{R}}{\operatorname{argmin}} \frac{1}{n+1} \sum_{i=1}^{n+1} \ell_\alpha(\theta \circ f_{n+1}^*(X_i), S_i).$$

The optimization problem defining ρ_{n+1}^* is intrinsically regularized since ρ_{n+1}^* is a transformation of the piece-wise constant function f_{n+1}^* and, therefore, must have the same number of constant segments as f_{n+1}^* . Notably, $\rho_{n+1}^*(X_{n+1})$ can be efficiently computed as the empirical $1 - \alpha$ quantile of the conformity scores within the same level set (or leaf) as X_{n+1} , that is, $\{S_i^* : f_{n+1}^*(X_i) = f_{n+1}^*(X_{n+1}), i \in [n+1]\}$. In the proof of Theorem 4.2 in the next section, we establish that $\mathbb{P}(Y_{n+1} \in C_{n+1}^*(X_{n+1}) \mid f_{n+1}^*(X_{n+1})) \geq 1 - \alpha$, i.e., the interval $C_{n+1}^*(X_{n+1})$ achieves desideratum (ii). To do so, similar to Gibbs et al. 2023, we leverage exchangeability and the first-order conditions of the convex optimization problem defining ρ_{n+1}^* to show that this prediction interval is *multi-calibrated* against the class of ‘covariate shifts’ $\mathcal{F}_{n+1} := \{\theta \circ f_{n+1}^*; \theta : \mathbb{R} \rightarrow \mathbb{R}\}$. In contrast with the multicalibration objective treated in Gibbs et al. 2023, \mathcal{F}_{n+1} is dependent on the calibration data through f_{n+1}^* , which presents additional challenges in our theoretical proofs.

Practical procedure. Our practical implementation of SC-CP, which is provided by Alg. 2, follows a similar procedure to the oracle method. Since the new outcome Y_{n+1} is unobserved, we instead iterate the oracle procedure over all possible imputed values $y \in \mathcal{Y}$ for Y_{n+1} . As in Algorithm 1., this yields a set of isotonic calibrated models $f_n^{(X_{n+1}, \diamond)} := \{f_n^{(X_{n+1}, y)} : y \in \mathcal{Y}\}$, where $f_n^{(X_{n+1}, \diamond)}(X_{n+1})$ is the Venn-Abers set prediction of Y_{n+1} . Next, for each $y \in \mathcal{Y}$ and $i \in [n]$, we define the *Venn-Abers conformity*

Algorithm 2 Self-Consistent Conformal Prediction

Input: Calibration data $\mathcal{C}_n = \{(X_1, Y_1), \dots, (X_n, Y_n)\}$, isotonic calibrator class Θ_{iso} , black-box model f , context $x \in \mathcal{X}$, and miscoverage level $\alpha \in (0, 1)$

- 1: **for** each $y \in \mathcal{Y}$ **do**
- 2: Obtain calibrated model $f_n^{(x,y)}$ by isotonic calibrating f on $\mathcal{C}_n \cup \{(x, y)\}$ using Θ_{iso} as in Alg. 1;
- 3: Set Venn-Abers conformity scores $S_i^{(x,y)} = |Y_i - f_n^{(x,y)}(X_i)|, \forall i \in [n]$ and $S_{n+1}^{(x,y)} = |y - f_n^{(x,y)}(x)|$;
- 4: Calculate the $1 - \alpha$ empirical quantile $\rho_n^{(x,y)}(x)$ of conformity scores with same calibrated prediction as x :

$$\operatorname{argmin}_{q \in \mathbb{R}} \sum_{i=1}^n K_i(f_n^{(x,y)}, x) \cdot \ell_\alpha(q, S_i^{(x,y)}) + \ell_\alpha(q, S_{n+1}^{(x,y)});$$

where $K_i(f_n^{(x,y)}, x) = \mathbf{1}\{f_n^{(x,y)}(X_i) = f_n^{(x,y)}(x)\}$.

5: **end for**

- 6: Set $\widehat{C}_n(x) := \{y \in \mathcal{Y} : |y - f_n^{(x,y)}(x)| \leq \rho_n^{(x,y)}(x)\}$.

Output: $\{f_n^{(x,y)}(x) : y \in \mathcal{Y}\} \subset \operatorname{conv}(\mathcal{Y}), \widehat{C}_n(x) \subset \mathcal{Y}$

scores $S_i^{(X_{n+1}, y)} := |Y_i - f_n^{(X_{n+1}, y)}(X_i)|$ and $S_{n+1}^{(X_{n+1}, y)} := |y - f_n^{(X_{n+1}, y)}(X_{n+1})|$. Our SC-CP interval is then given by $\widehat{C}_n(X_{n+1}) := \{y \in \mathcal{Y} : S_{n+1}^{(X_{n+1}, y)} \leq \rho_n^{(X_{n+1}, y)}(X_{n+1})\}$, where $\rho_n^{(X_{n+1}, y)}(X_{n+1})$ is the empirical $1 - \alpha$ quantile of the level set $\{S_i^{(X_{n+1}, y)} : f_n^{(X_{n+1}, y)}(X_i) = f_n^{(X_{n+1}, y)}(X_{n+1}), i \in [n+1]\}$. By definition, our interval $\widehat{C}_n(X_{n+1})$ covers Y_{n+1} if, and only if, the oracle interval $C_{n+1}^*(X_{n+1})$ covers Y_{n+1} . Formally, $\widehat{C}_n(X_{n+1})$ is a set, but it can always be converted to an interval by taking its range at a negligible cost in efficiency.

Computational considerations. Alg. 2 must be applied separately for every context $x \in \mathcal{X}$ for which a calibrated prediction is desired. As in the discussion of Alg. 1, the computational complexity of SC-CP can be reduced by discretizing the prediction space $f(\mathcal{X}) = \{f(x) : x \in \mathcal{X}\} \subset \mathbb{R}$. Similar to Full CP (Vovk et al., 2005), Alg. 2 may be infeasible to compute exactly for non-discrete outcomes, and in such cases, it can be approximated by discretizing \mathcal{Y} . If $f(\mathcal{X})$ and \mathcal{Y} are each discretized into $j \in \mathbb{N}$ bins, to compute predictions across all $x \in \mathcal{X}$ and $y \in \mathcal{Y}$, Alg. 2 requires the computation of j^2 isotonic regression solutions, where each regression can be computed in linear time. In our experiments, for each $x \in \mathcal{X}$, we found computing $\rho_n^{(x,y)}(x)$ over a finite grid of \mathcal{Y} and then linearly interpolating over non-grid points effectively mitigated approximation error. With calibration and test datasets of size $n = 5000$, we found quantile binning both $f(\mathcal{X})$ and \mathcal{Y} into 200 equal-frequency bins and using linear interpolation over \mathcal{Y} allows us to execute Alg. 2 across all contexts in the test data in a few minutes with negligible approximation error.

4 Theoretical guarantees

In this section, we establish that, under no distributional assumptions and in finite samples, the Venn-Abers set prediction and SC-CP interval output by Alg. 2 satisfy desiderata (i) and (ii). We do so under an assumption weaker than *iid*, namely, exchangeability of the calibration data \mathcal{C}_n and new data point (X_{n+1}, Y_{n+1}) . Under an *iid* condition and with sufficient calibration data, we further establish that the

Venn-Abers calibration step within the SC-CP algorithm typically results in better point predictions and conformity scores and, consequently, more efficient prediction intervals.

The following theorem establishes that the Venn-Abers set prediction $f_n^{(X_{n+1}, \diamond)}(X_{n+1}) := \{f_n^{(X_{n+1}, y)}(X_{n+1}) : y \in \mathcal{Y}\}$ contains a self-consistent point prediction of Y_{n+1} .

C1) *Exchangeability:* $\{(X_i, Y_i)\}_{i=1}^{n+1}$ are exchangeable.

C2) *Finite second moment:* $E_P[Y^2] < \infty$.

Theorem 4.1 (Self-consistency of Venn-Abers predictions). *Under Conditions C1 and C2, the Venn-Abers set prediction $f_n^{(X_{n+1}, \diamond)}(X_{n+1})$ almost surely satisfies the condition $f_n^{(X_{n+1}, Y_{n+1})}(X_{n+1}) = \mathbb{E}[Y_{n+1} \mid f_n^{(X_{n+1}, Y_{n+1})}(X_{n+1})]$.*

While the result of Theorem 4.1 is identical to the result proven by Vovk and Petej 2012 in the special case of the classification setup, our proof is novel and elucidates how Venn-Abers calibration uses exchangeability with the least-squares loss in a manner completely analogous to how conformal prediction uses exchangeability with the quantile loss (Gibbs et al., 2023). The self-consistent prediction $f_n^{(X_{n+1}, Y_{n+1})}(X_{n+1})$ can typically not be determined precisely, without knowledge of Y_{n+1} . However, the stability of isotonic regression implies the width of $f_n^{(X_{n+1}, \diamond)}(X_{n+1})$ shrinks towards zero as the size of the calibration set increases (Caponnetto and Rakhlin, 2006). Notably, the large-sample theory for isotonic calibration, developed in van der Laan et al. 2023, demonstrates that the ℓ^2 -calibration error (Gupta et al., 2020) of any point prediction within the set $f_n^{(X_{n+1}, \diamond)}(X_{n+1})$ asymptotically approaches zero at a dimensionless rate of $n^{-2/3}$.

The following theorem establishes self-consistency and, thereby, desideratum (ii) for the SC-CP interval $\widehat{C}_n(X_{n+1})$ with respect to the (self-consistent) oracle Venn-Abers prediction $f_n^{(X_{n+1}, Y_{n+1})}(X_{n+1})$. In the following conditions and theorem, we let $\text{polylog}(n)$ be a fixed, given sequence that grows polynomially logarithmically in n . For $i \in [n+1]$, we recall that $S_i^{(X_{n+1}, Y_{n+1})} := |Y_i - f_n^{(X_{n+1}, Y_{n+1})}(X_i)|$.

C3) *Isotonic regression tree is not too deep:* The number of constant segments for $f_n^{(X_{n+1}, Y_{n+1})}$ is at most $n^{1/3} \text{polylog}(n)$.

C4) *No ties:* The conformity scores $S_i^{(X_{n+1}, Y_{n+1})}$, $\forall i \in [n+1]$, are almost surely distinct.

Theorem 4.2 (Self-consistency of prediction interval). *Under C1, it holds almost surely that*

$$\mathbb{P}\left(Y_{n+1} \in \widehat{C}_n(X_{n+1}) \mid f_n^{(X_{n+1}, Y_{n+1})}(X_{n+1})\right) \geq 1 - \alpha.$$

If also C3 and C4 hold, then the coverage deviation satisfies:

$$\mathbb{E}\left|\alpha - \mathbb{P}\left(Y_{n+1} \notin \widehat{C}_n(X_{n+1}) \mid f_n^{(X_{n+1}, Y_{n+1})}(X_{n+1})\right)\right| \leq \frac{\text{polylog}(n)}{n^{2/3}}.$$

One caveat of SC-CP is that desideratum (ii) is satisfied with respect to the unknown, oracle Venn-Abers prediction $f_n^{(X_{n+1}, Y_{n+1})}(X_{n+1})$. However, by Theorem 4.1, we know that this oracle point prediction lies within the Venn-Abers set prediction and its value can be precisely determined as the size of the calibration set increases asymptotically. The second part of Theorem 4.2 says that $\widehat{C}_n(X_{n+1})$ satisfies desideratum (ii) with coverage that is, on average, conservative up to a factor $\frac{\text{polylog}(n)}{n^{2/3}}$. Notably, the deviation error from exact coverage tends to zero at a fast rate, irrespective of the dimension d of the context X_{n+1} . Consequently, we find that self-consistency is a much more attainable property than (2), since the latter suffers from the “curse of dimensionality” (Gibbs et al., 2023).

The leaf growth rate of $n^{1/3} \text{polylog}(n)$ imposed in C3 is motivated by the theoretical properties of isotonic regression, and we note our proof and theorem statement can be adapted to allow for any leaf growth rate $c(n) \uparrow \infty$. Condition C3 can always be guaranteed to hold by constraining the maximum number of constant segments $k(n) \in \mathbb{N} \cup \{\infty\}$ of functions in the calibrator class Θ_{iso} . These constraints can be enforced using the maximum tree depth and minimum leaf node size arguments of commonly-available implementations of `xgboost` (Chen and Guestrin, 2016). However, even without constraints ($k(n) = \infty$), we expect this condition to hold under fairly weak assumptions. For example, assuming the outcomes have finite variance and $t \mapsto E_P[Y \mid f(X) = t]$ is continuously differentiable, Deng et al. 2021 show that the number of observations in a given constant segment of a univariate isotonic regression tree concentrates in probability around $n^{2/3}$ — see Lemma 1. of Dai et al. 2020 for a related result. Condition C4 is only required to establish the upper coverage bound and is standard in CP - see, e.g., Li et al. 2018; Gibbs et al. 2023. Since $f_n^{(X_{n+1}, Y_{n+1})}$ is piece-wise constant, this condition is usually violated for discrete outcomes. This condition can be avoided by adding a small amount of noise to all outcomes (Li et al., 2018).

The next theorem examines the interaction between Venn-Abers calibration and CP within the SC-CP procedure in terms of efficiency of the Venn-Abers conformity scores.

- C5)** *Calibrator class Θ_{iso} is maximal: $k(n) = \infty$.*
- C6)** *Independent data: $\{(X_i, Y_i)\}_{i=1}^{n+1}$ are iid.*
- C7)** *Bounded outcomes: \mathcal{Y} is a uniformly bounded set.*

For each $\theta \in \Theta_{\text{iso}}$, define the θ -transformed conformity scoring function $S_\theta : (x, y) \mapsto |y - \theta \circ f(x)|$. Let $\theta_0 := \text{argmin}_{\theta \in \Theta_{\text{iso}}} \int \{S_\theta(x', y')\}^2 dP(x', y')$ be the optimal isotonic transformation of $f(\cdot)$ that minimizes the population mean-square error and, hence, corresponds to a conformity score of minimal second moment. Define the Venn-Abers conformity scoring function as $S_n^{(x, y)}(x, y) := |y - f_n^{(x, y)}(x)|$, where $f_n^{(x, y)}$ is obtained as in Alg. 1.

Theorem 4.3. *Under C5-C7, it holds, for any $x \in \mathcal{X}, y \in \mathcal{Y}$, that*

$$\int \{S_n^{(x,y)}(x', y') - S_{\theta_0}(x', y')\}^2 dP(x', y') = O_p(n^{-2/3}).$$

The above theorem indicates that the Venn-Abers scoring function $S_n^{(x,y)}$ used in Alg. 2 asymptotically converges in mean-square error to the oracle scoring function S_{θ_0} at a rate of $n^{-2/3}$. Since the oracle scoring function S_{θ_0} corresponds to a model $\theta_0 \circ f$ with better mean square error than f (by C5), we heuristically expect that the Venn-Abers scoring function $S_n^{(x,y)}$ will translate to narrower CP intervals, at least asymptotically. We provide experimental evidence for this heuristic in Section 5.2.

4.1 Related work

The impossibility results of Gupta et al. 2020 establish that self-consistency in desideratum (ii) can only be achieved when the output space $f(\mathcal{X})$ is discrete. Consequently, any universal procedure providing self-consistent intervals must explicitly or implicitly apply some form of output discretization. Johansson et al. 2014 and Johansson et al. 2018 propose conformal regression trees, which apply Mondrian CP (Vovk et al., 2005) within leaves of a regression tree f . They provide prediction intervals with valid coverage within the leaves of the tree, thereby satisfying desideratum (ii). However, this approach is restricted to tree-based predictors and generally does not guarantee calibrated point predictions. Boström et al. 2021 propose Mondrian conformal predictive distributions applied within bins of model predictions to satisfy a coarser, distributional form of desideratum (ii). A limitation of these Mondrian-CP approaches is that they require pre-specification of a binning scheme for the predictor $f(\cdot)$, which introduces a trade-off between model performance and the width of prediction intervals, and they do not perform point calibration in the sense of desideratum (i). In contrast, SC-CP data-adaptively discretizes the predictor $f(\cdot)$ using isotonic calibration and, in doing so, provides calibrated predictions (desideratum (i)) and improved conformity scores. The data-dependent nature of the discretization procedure used in SC-CP substantially complicates our theoretical analyses.

Other notions of conditional validity have been proposed that, like self-consistency, avoid the curse of dimensionality of context-conditional validity. In the multiclassification setup, Shi et al. 2013 and Ding et al. 2023 study class-conditional validity and use Mondrian CP to provide prediction intervals with valid coverage conditional on the class label (i.e., outcome). Boström and Johansson 2020 apply Mondrian CP within bins categorized by context-specific difficulty estimates, such as conditional variance estimates. Multivald-CP (Jung et al., 2022; Bastani et al., 2022) uses binning to provide coverage conditional on a threshold value

that defines the prediction interval. This ‘threshold calibration’ objective corresponds to a quantile form of desideratum (i) wherein the outcome predictor $f(\cdot)$ is replaced with a quantile predictor and means are replaced with quantiles — see Section 3.3. of Roth 2022 for further details on quantile calibration. For multiclassification, Noarov et al. 2023 propose a procedure for attaining valid coverage conditional on the prediction set size, a property dubbed *size-stratified coverage validity* (Angelopoulos et al., 2020).

5 Experiments

5.1 Experimental setup

Synthetic datasets. We construct synthetic training, calibration, and test datasets \mathcal{D}_{train} , \mathcal{D}_{cal} , \mathcal{D}_{test} of sizes $n_{train}, n_{cal}, n_{test}$, which are respectively used to train f , apply CP, and evaluate performance. For parameters $d \in \mathbb{N}, \kappa > 0, a \geq 0, b \geq 0$, each dataset consists of *iid* observations of (X, Y) drawn as follows. The covariate vector $X := (X_1, \dots, X_d) \in [0, 1]^d$ is coordinate-wise independently drawn from a Beta($1, \kappa$) distribution with shape parameter κ . Then, conditionally on $X = x$, the outcome Y is drawn normally distributed with conditional mean $\mu(x) := \frac{1}{d} \sum_{j=1}^d \{x_j + \sin(4x_j)\}$ and conditional variance $\sigma^2(x) := \{0.035 + ag(x) + b(|\mu_0(x)|^6/20 - 0.02)\}^2$, where $g(x) := -\log(0.5 + 0.5x_1)/4$. Here, a and b control the heteroscedasticity and mean-variance relationship for the outcomes. For \mathcal{D}_{cal} and \mathcal{D}_{test} , we set $\kappa_{cal} = \kappa_{test} = 1$ and, for \mathcal{D}_{train} , we vary κ_{train} to introduce distribution shift and, thereby, calibration error in f . The parameters d , a , and b are fixed across the datasets.

Baselines. To mitigate overfitting, we implement SC-CP so that each function in Θ_{iso} has at least 20 observations averaged within each constant segment (implemented using the minimum leaf node size of argument `xgboost`). When appropriate, we will consider the following baseline CP algorithms for comparison. Unless stated otherwise, for all baselines, we use the scoring function $S(x, y) := |y - f(x)|$. The first baseline, uncond-CP, is split-CP (Li et al., 2018), which provides only unconditional coverage guarantees. The second baseline, cond-CP, is adapted from Gibbs et al. 2023 and provides conditional coverage over distribution shifts within a specified reproducing kernel Hilbert space. Following Section 5.1 of Gibbs et al. 2023, we use the Gaussian kernel $K(X_i, X_j) := \exp(-4\|X_i - X_j\|_2^2)$ with euclidean norm $\|\cdot\|_2$ and select the regularization parameter λ using 5-fold cross-validation. The third baseline, Mondrian CP, applies the Mondrian CP method (Vovk et al., 2005; Boström and Johansson, 2020) to categories formed by dividing f ’s predictions into 20 equal-frequency bins based on \mathcal{D}_{cal} . As an optimal benchmark, we consider the oracle satisfying (2).

5.2 Experiment 1: Calibration and efficiency

In this experiment, we illustrate how calibration of the predictor f can improve the efficiency (i.e., width) of the resulting prediction intervals. We consider the data-generating process of the previous section, with $n_{train} = n_{cal} = n_{test} = 1000$, $d = 5$, $a = 0$, and $b = 0.6$. The predictor f is trained on \mathcal{D}_{train} using the *ranger* (Wright and Ziegler, 2017) implementation of random forests with default settings. To control the calibration error in f , we vary the distribution shift parameter κ_{train} for \mathcal{D}_{train} over $\{1, 1.5, 2, 2.5, 3\}$.

Results. Figure 2a compares the average interval width across \mathcal{D}_{test} for SC-CP and baselines as the ℓ^2 -calibration error in f increases. Here, we estimate the calibration error using the approach of Xu and Yadlowsky 2022. As calibration error increases, the average interval width for SC-SP appears smaller than those of uncond-CP, Mondrian-CP, and cond-CP, especially in comparison to uncond-CP. The observed efficiency gains in SC-CP are consistent with Theorem 4.3 and provides empirical evidence that Venn-Abers conformity scores translate to tighter prediction intervals, given sufficient data. To test this hypothesis under controlled conditions, we compare the widths of prediction intervals obtained using vanilla (unconditional) CP for two scoring functions: $S : (x, y) \mapsto |y - f(x)|$ and the Venn-Abers (worst-case) scoring function $S_{cal} : (x, y) \mapsto \max_{y \in \mathcal{Y}} |y - f_n^{(x,y)}(x)|$. For miscoverage levels $\alpha \in \{0.05, 0.1, 0.2\}$, the left panel of Figure 2b illustrates the relative efficiency gain achieved by using S_{cal} , which we define as the ratio of the average interval widths for S_{cal} relative to S . The widths and calibration errors in Figure 2b are averaged across 100 data replicates.

Role of calibration set size. With too small calibration sets, the isotonic calibration step in Alg. 2 can lead to overfitting. In such cases, the Venn-Abers conformity scores could be larger than their uncalibrated counterparts, potentially resulting in less efficient prediction intervals. In our experiments, overfitting is mitigated by constraining the minimum size of the leaf node in the isotonic regression tree to 20. For $\alpha \in \{0.05, 0.1, 0.2\}$, the right panel of Figure 2b displays the relationship between n_{cal} and the relative efficiency gain achieved by using S_{cal} , holding calibration error fixed ($\kappa_{train} = 3$). We find that calibration leads to a noticeable reduction in interval width as soon as $n_{cal} \geq 50$.

5.3 Experiment 2: Coverage and Adaptivity

In this experiment, we illustrate how self-consistency of $\widehat{C}_n(X_{n+1})$ can, in some cases, translate to stronger conditional coverage guarantees. Here we take $n_{train} = n_{cal} = 1000$ and $n_{test} = 2500$, and no distribution shift ($\kappa_{train} = 1$) in \mathcal{D}_{train} . We consider three setups: **Setup A** ($d = 5, a = 0, b = 0.6$) and **Setup B** ($d = 5, a = 0, b = 0.6$) which have a strong mean-variance relationship in the outcome process; and **Setup C** ($d = 5, a = 0.6, b = 0$) which has no such relationship. We obtain the predictor f from \mathcal{D}_{train} using a generalized additive model (Hastie and Tibshirani, 1987), so that it is well calibrated and accurately estimates

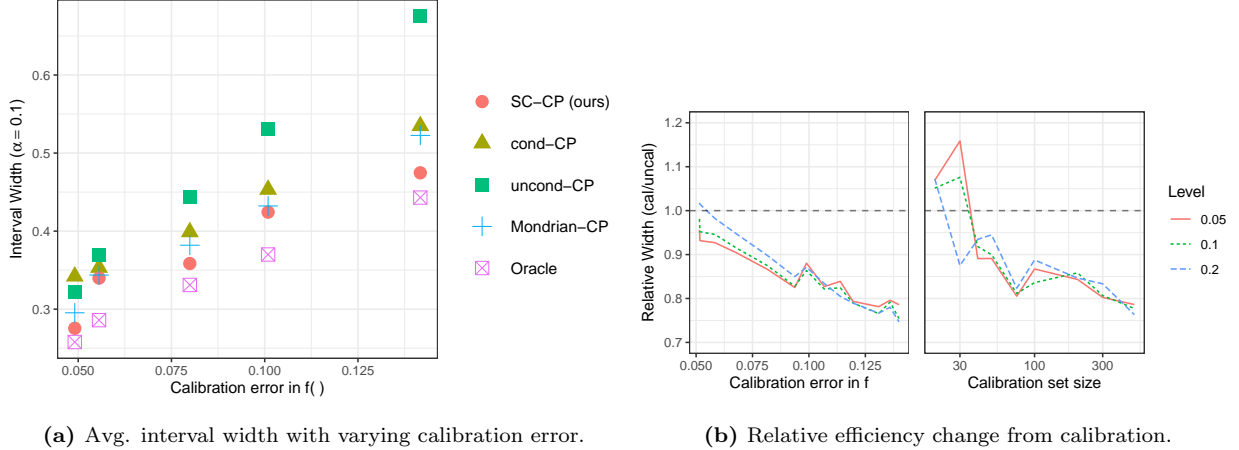


Figure 2: Figure 2a shows the average interval widths for varying ℓ^2 -calibration errors in f . Figure 2b shows the relative change in average interval width using Venn-Abers calibrated versus uncalibrated predictions, with varying ℓ^2 -calibration error in f (left), and calibration set size (right). Below the horizontal lines signifies efficiency gains for SC-CP.

μ . To assess the adaptivity of SC-CP to heteroscedasticity, we report the coverage and the average interval width within subgroups of \mathcal{D}_{test} defined by quintiles of the conditional variances $\{\sigma^2(X_i) : (X_i, Y_i) \in \mathcal{D}_{test}\}$.

Results. The top two panels in Figure 3a displays the coverage and average interval width results for **Setup A** and **Setup B**. In both setups, SC-CP, cond-CP, and Mondrian-CP exhibit satisfactory coverage both marginally and within the quintile subgroups. In contrast, while uncond-CP attains the nominal level of marginal coverage, it exhibits noticeable overcoverage within the first three quintiles and significant undercoverage within the fifth quintile. The satisfactory performance of SC-CP with respect to heteroscedasticity in **Setups A and B** can be attributed to the strong mean-variance relationship in the outcome process. Regarding efficiency, the average interval widths of SC-CP are competitive with those of prediction-binned Mondrian-CP and the oracle intervals. The interval widths for cond-CP are wider than those for SC-CP and Mondrian-CP, especially for **Setup B**. This difference can be explained by cond-CP aiming for conditional validity in a 5D and 20D space, whereas SC-CP and Mondrian-CP target the 1D output space.

Limitation. If there is no mean-variance relationship in the outcomes, SC-CP is generally not expected to adapt to heteroscedasticity. The third (bottom) panel of Figure 3a displays SC-CP’s performance in **Setup C**, where there is no such relationship. In this scenario, it is evident that the conditional coverage of both uncond-CP and SC-CP are poor, while cond-CP maintains adequate coverage.

Adaptivity and calibration set size. SC-CP can be derived by applying CP within subgroups defined by a data-dependent binning of the output space $f(\mathcal{X})$, learned via Venn-Abers calibration, where the number of bins can grow with n_{cal} . In particular, if $t \mapsto E[Y | f(X) = t]$ is asymptotically monotone, which is plausible when f consistently estimates the outcome regression, then the number of bins selected by isotonic calibration will generally increase with n_{cal} , and the width of these bins will tend to zero. As a

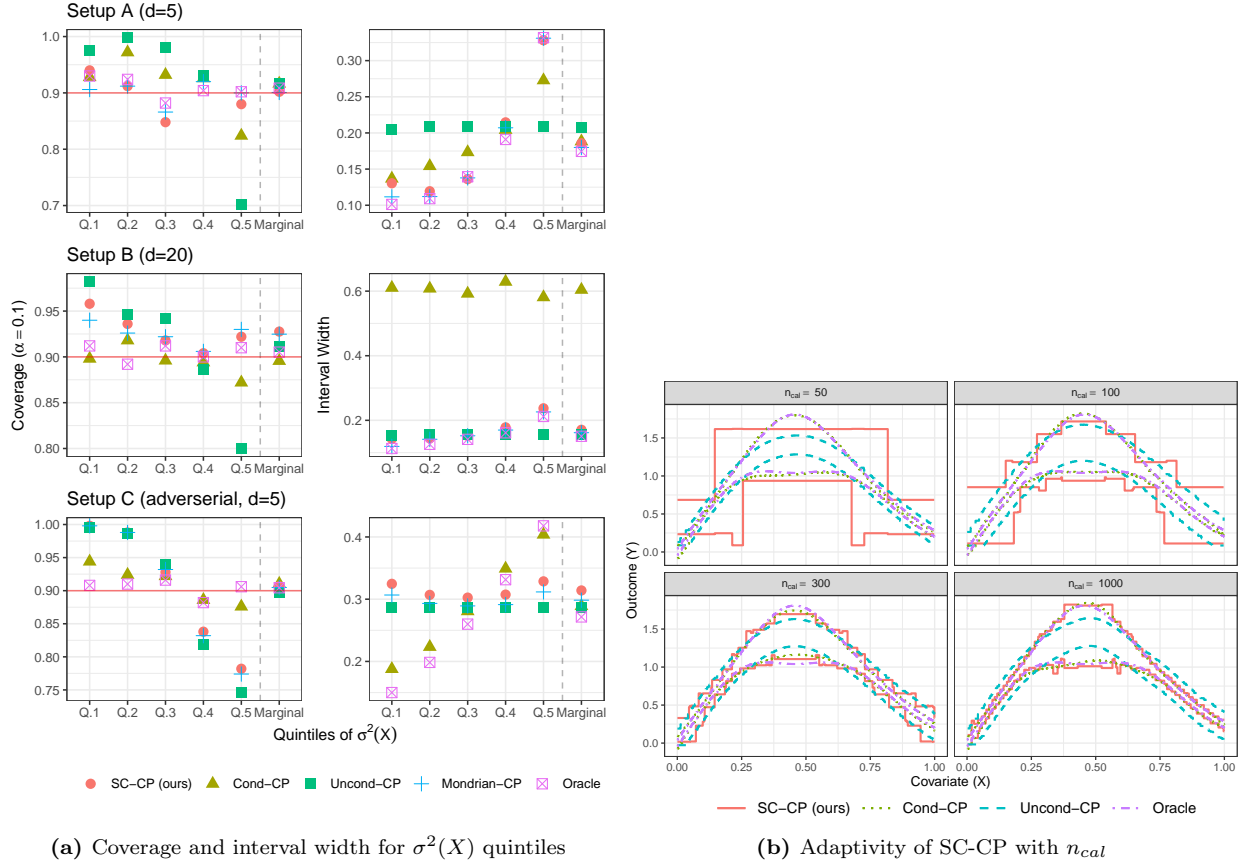


Figure 3: Figure 3a displays the coverage and average interval width of SC-CP, marginally and within quintiles of the conditional outcome variance for setups A, B, and C. For a $d = 1$ example, Figure 3b shows the adaptivity of SC-CP prediction bands ($\alpha = 0.1$) across various calibration set sizes.

consequence, in such cases, the self-consistency result in Theorem 4.2 translates to conditional guarantees over finer partitions of $f(\mathcal{X})$ as n_{cal} increases. For $d = 1$ and a strong mean-variance relationship ($a = 0, b = 0.6$), Figure 3b demonstrates how the adaptivity of SC-CP bands improves as n_{cal} increases. In this case, for n_{cal} sufficiently large, we find that the SC-CP bands closely match those of cond-CP and the oracle.

6 Conclusion

In this work, we propose a dual-calibration objective (desiderata (i) and (ii)) for providing self-consistent point predictions and prediction intervals. After proposing an oracle procedure for achieving (i) and (ii), we develop SC-CP, a method that combines two post-hoc approaches: Venn-Abers calibration (Vovk and Petej, 2012) and split CP (Lei et al., 2018). SC-CP has some caveats. The first caveat is that, instead of providing a single point prediction, SC-CP provides a set of point predictions that almost surely includes a point prediction meeting (i) in finite samples. However, this set prediction converges asymptotically to a

single self-consistent point prediction. The second caveat is that SC-CP satisfies (ii) in finite samples with respect to an unknown, oracle point prediction. Nonetheless, this oracle point prediction lies within the Venn-Abers set prediction and can be precisely determined asymptotically. Regarding extensions of SC-CP, it might be beneficial to attain self-consistency within user-specified subgroups. Achieving a group-valid form of SC-CP is possible by separately applying Algorithm 2 within each subgroup, as in Multivald CP (Jung et al., 2022). Additionally, while we use isotonic calibration, Alg. 2 could be modified to use other binning calibration methods, such as Venn calibration (Vovk and Petej, 2012), by replacing the isotonic regression step in Alg. 1 with, e.g., quantile binning.

References

- A. Angelopoulos, S. Bates, J. Malik, and M. I. Jordan. Uncertainty sets for image classifiers using conformal prediction. *arXiv preprint arXiv:2009.14193*, 2020.
- V. Balasubramanian, S.-S. Ho, and V. Vovk. *Conformal prediction for reliable machine learning: theory, adaptations and applications*. Newnes, 2014.
- R. Barber, E. J. Candes, A. Ramdas, and R. J. Tibshirani. The limits of distribution-free conditional predictive inference. *Information and Inference: A Journal of the IMA*, 10(2):455–482, 2021.
- R. E. Barlow and H. D. Brunk. The isotonic regression problem and its dual. *Journal of the American Statistical Association*, 67(337):140–147, 1972.
- O. Bastani, V. Gupta, C. Jung, G. Noarov, R. Ramalingam, and A. Roth. Practical adversarial multivald conformal prediction. *Advances in Neural Information Processing Systems*, 35:29362–29373, 2022.
- A. Bella, C. Ferri, J. Hernández-Orallo, and M. J. Ramírez-Quintana. Calibration of machine learning models. In *Handbook of Research on Machine Learning Applications and Trends: Algorithms, Methods, and Techniques*, pages 128–146. IGI Global, 2010.
- R. Bhardwaj, A. R. Nambiar, and D. Dutta. A study of machine learning in healthcare. In *2017 IEEE 41st annual computer software and applications conference (COMPSAC)*, volume 2, pages 236–241. IEEE, 2017.
- H. Boström and U. Johansson. Mondrian conformal regressors. In *Conformal and Probabilistic Prediction and Applications*, pages 114–133. PMLR, 2020.
- H. Boström, U. Johansson, and T. Löfström. Mondrian conformal predictive distributions. In *Conformal and Probabilistic Prediction and Applications*, pages 24–38. PMLR, 2021.

- A. Caponnetto and A. Rakhlin. Stability properties of empirical risk minimization over donsker classes. *Journal of Machine Learning Research*, 7(12), 2006.
- D. S. Char, N. H. Shah, and D. Magnus. Implementing machine learning in health care—addressing ethical challenges. *The New England journal of medicine*, 378(11):981, 2018.
- T. Chen and C. Guestrin. XGBoost: A scalable tree boosting system. In *Proceedings of the 22nd ACM SIGKDD International Conference on Knowledge Discovery and Data Mining*, KDD '16, pages 785–794, New York, NY, USA, 2016. ACM. ISBN 978-1-4503-4232-2. doi: 10.1145/2939672.2939785. URL <http://doi.acm.org/10.1145/2939672.2939785>.
- R. Dai, H. Song, R. F. Barber, and G. Raskutti. The bias of isotonic regression. *Electronic journal of statistics*, 14(1):801, 2020.
- S. E. Davis, T. A. Lasko, G. Chen, E. D. Siew, and M. E. Matheny. Calibration drift in regression and machine learning models for acute kidney injury. *Journal of the American Medical Informatics Association*, 24(6):1052–1061, 2017.
- H. Deng, Q. Han, and C.-H. Zhang. Confidence intervals for multiple isotonic regression and other monotone models. *The Annals of Statistics*, 49(4):2021–2052, 2021.
- Z. Deng, C. Dwork, and L. Zhang. Happymap: A generalized multi-calibration method. *arXiv preprint arXiv:2303.04379*, 2023.
- T. Ding, A. N. Angelopoulos, S. Bates, M. I. Jordan, and R. J. Tibshirani. Class-conditional conformal prediction with many classes. *arXiv preprint arXiv:2306.09335*, 2023.
- B. Efron. The two sample problem with censored data. In *Proceedings of the fifth Berkeley symposium on mathematical statistics and probability*, volume 4, pages 831–853, 1967.
- G. Feretzakis, A. Sakagianni, E. Loupelis, D. Kalles, N. Skarmoutsou, M. Martsoukou, C. Christopoulos, M. Lada, S. Petropoulou, A. Velentza, et al. Machine learning for antibiotic resistance prediction: A prototype using off-the-shelf techniques and entry-level data to guide empiric antimicrobial therapy. *Healthcare informatics research*, 27(3):214, 2021.
- B. Flury and T. Tarpey. Self-consistency: A fundamental concept in statistics. *Statistical Science*, 11(3):229–243, 1996.
- I. Gibbs, J. J. Cherian, and E. J. Candès. Conformal prediction with conditional guarantees. *arXiv preprint arXiv:2305.12616*, 2023.

- P. Groeneboom and H. Lopuhaa. Isotonic estimators of monotone densities and distribution functions: basic facts. *Statistica Neerlandica*, 47(3):175–183, 1993.
- L. Guan. Localized conformal prediction: A generalized inference framework for conformal prediction. *Biometrika*, 110(1):33–50, 2023.
- C. Guo, G. Pleiss, Y. Sun, and K. Q. Weinberger. On calibration of modern neural networks. In *International conference on machine learning*, pages 1321–1330. PMLR, 2017.
- C. Gupta and A. Ramdas. Distribution-free calibration guarantees for histogram binning without sample splitting. In *International Conference on Machine Learning*, pages 3942–3952. PMLR, 2021.
- C. Gupta, A. Podkopaev, and A. Ramdas. Distribution-free binary classification: prediction sets, confidence intervals and calibration. *Advances in Neural Information Processing Systems*, 33:3711–3723, 2020.
- T. Hastie and R. Tibshirani. Generalized additive models: some applications. *Journal of the American Statistical Association*, 82(398):371–386, 1987.
- T. Heskes. Practical confidence and prediction intervals. *Advances in neural information processing systems*, 9, 1996.
- R. Hore and R. F. Barber. Conformal prediction with local weights: randomization enables local guarantees. *arXiv preprint arXiv:2310.07850*, 2023.
- Y. Jin and Z. Ren. Confidence on the focal: Conformal prediction with selection-conditional coverage. *arXiv preprint arXiv:2403.03868*, 2024.
- U. Johansson, C. Sönströd, H. Linusson, and H. Boström. Regression trees for streaming data with local performance guarantees. In *2014 IEEE International Conference on Big Data (Big Data)*, pages 461–470. IEEE, 2014.
- U. Johansson, H. Linusson, T. Löfström, and H. Boström. Interpretable regression trees using conformal prediction. *Expert systems with applications*, 97:394–404, 2018.
- U. Johansson, T. Löfström, and C. Sönströd. Well-calibrated probabilistic predictive maintenance using venn-abers. *arXiv preprint arXiv:2306.06642*, 2023.
- C. Jung, G. Noarov, R. Ramalingam, and A. Roth. Batch multivalid conformal prediction. *arXiv preprint arXiv:2209.15145*, 2022.

- J. Kang, R. Schwartz, J. Flickinger, and S. Beriwal. Machine learning approaches for predicting radiation therapy outcomes: a clinician’s perspective. *International Journal of Radiation Oncology* Biology* Physics*, 93(5):1127–1135, 2015.
- C.-I. C. Lee. The min-max algorithm and isotonic regression. *The Annals of Statistics*, 11(2):467–477, 1983.
- J. Lei and L. Wasserman. Distribution-free prediction bands for non-parametric regression. *Journal of the Royal Statistical Society Series B: Statistical Methodology*, 76(1):71–96, 2014.
- J. Lei, M. G’Sell, A. Rinaldo, R. J. Tibshirani, and L. Wasserman. Distribution-free predictive inference for regression. *Journal of the American Statistical Association*, 113(523):1094–1111, 2018.
- Y. Li, L. Qi, and Y. Sun. Semiparametric varying-coefficient regression analysis of recurrent events with applications to treatment switching. *Statistics in Medicine*, 37:3959–3974, 2018. doi: 10.1002/sim.7856. PubMed PMID: 29992591. NIHMSID: NIHMS1033642.
- E. B. Mandinach, M. Honey, and D. Light. A theoretical framework for data-driven decision making. In *annual meeting of the American Educational Research Association, San Francisco, CA*, 2006.
- B. Marr. *Artificial intelligence in practice: how 50 successful companies used AI and machine learning to solve problems*. John Wiley & Sons, 2019.
- A. Niculescu-Mizil and R. Caruana. Obtaining calibrated probabilities from boosting. In *UAI*, volume 5, pages 413–20, 2005.
- G. Noarov, R. Ramalingam, A. Roth, and S. Xie. High-dimensional prediction for sequential decision making. *arXiv preprint arXiv:2310.17651*, 2023.
- J. Patel. Prediction intervals-a review. *Communications in Statistics-Theory and Methods*, 18(7):2393–2465, 1989.
- J. Platt et al. Probabilistic outputs for support vector machines and comparisons to regularized likelihood methods. *Advances in large margin classifiers*, 10(3):61–74, 1999.
- L. Quest, A. Charrie, L. du Croo de Jongh, and S. Roy. The risks and benefits of using ai to detect crime. *Harv. Bus. Rev. Digit. Artic*, 8:2–5, 2018.
- Y. Romano, R. F. Barber, C. Sabatti, and E. Candès. With malice toward none: Assessing uncertainty via equalized coverage. *Harvard Data Science Review*, 2(2):4, 2020.
- A. Roth. *Uncertain: Modern topics in uncertainty estimation*, 2022.

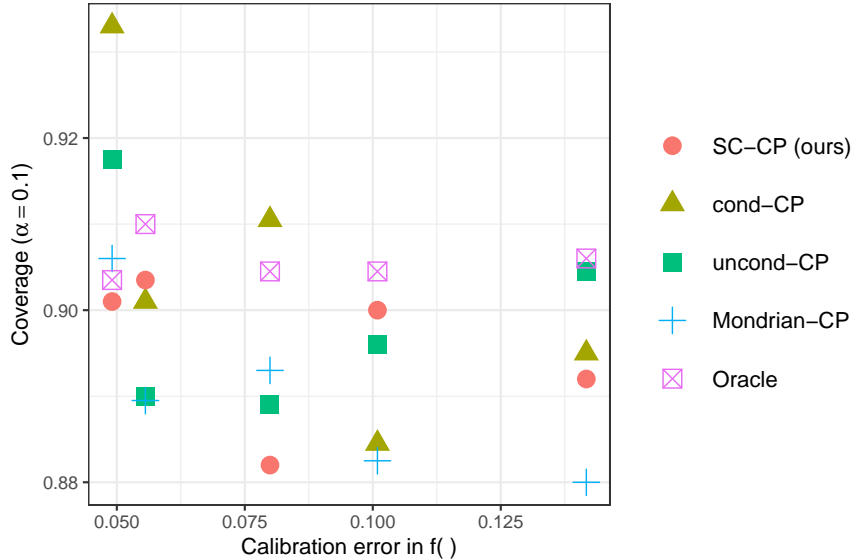
- A. Sakagianni, C. Koufopoulou, G. Feretzakis, D. Kalles, V. S. Verykios, and P. Myriantsefs. Using machine learning to predict antimicrobial resistance—a literature review. *Antibiotics*, 12(3):452, 2023.
- M. Sesia and Y. Romano. Conformal prediction using conditional histograms. *Advances in Neural Information Processing Systems*, 34:6304–6315, 2021.
- G. Shafer and V. Vovk. A tutorial on conformal prediction. *Journal of Machine Learning Research*, 9(3), 2008.
- F. Shi, C. S. Ong, and C. Leckie. Applications of class-conditional conformal predictor in multi-class classification. In *2013 12th International Conference on Machine Learning and Applications*, volume 1, pages 235–239. IEEE, 2013.
- R. J. Tibshirani, R. Foygel Barber, E. Candès, and A. Ramdas. Conformal prediction under covariate shift. *Advances in neural information processing systems*, 32, 2019.
- L. van der Laan, E. Ulloa-Pérez, M. Carone, and A. Luedtke. Causal isotonic calibration for heterogeneous treatment effects. In *Proceedings of the 40th International Conference on Machine Learning (ICML)*, volume 202, Honolulu, Hawaii, USA, 2023. PMLR.
- L. van der Laan, E. Ulloa-Pérez, M. Carone, and A. Luedtke. Causal isotonic calibration for heterogeneous treatment effects. *arXiv preprint arXiv:2302.14011*, 2023.
- A. van der Vaart and J. Wellner. *Weak Convergence and Empirical Processes*. Springer, New York, 1996.
- A. Van Der Vaart and J. A. Wellner. A local maximal inequality under uniform entropy. *Electronic Journal of Statistics*, 5(2011):192, 2011.
- V. Vapnik, E. Levin, and Y. Le Cun. Measuring the vc-dimension of a learning machine. *Neural computation*, 6(5):851–876, 1994.
- J. Vazquez and J. C. Facelli. Conformal prediction in clinical medical sciences. *Journal of Healthcare Informatics Research*, 6(3):241–252, 2022.
- M. Veale, M. Van Kleek, and R. Binns. Fairness and accountability design needs for algorithmic support in high-stakes public sector decision-making. In *Proceedings of the 2018 chi conference on human factors in computing systems*, pages 1–14, 2018.
- V. Vovk. Conditional validity of inductive conformal predictors. In *Asian conference on machine learning*, pages 475–490. PMLR, 2012.

- V. Vovk and I. Petej. Venn-abers predictors. *arXiv preprint arXiv:1211.0025*, 2012.
- V. Vovk, A. Gammerman, and G. Shafer. *Algorithmic learning in a random world*, volume 29. Springer, 2005.
- M. N. Wright and A. Ziegler. ranger: A fast implementation of random forests for high dimensional data in C++ and R. *Journal of Statistical Software*, 77(1):1–17, 2017. doi: 10.18637/jss.v077.i01.
- Y. Xu and S. Yadlowsky. Calibration error for heterogeneous treatment effects. In *International Conference on Artificial Intelligence and Statistics*, pages 9280–9303. PMLR, 2022.
- B. Zadrozny and C. Elkan. Obtaining calibrated probability estimates from decision trees and naive bayesian classifiers. In *Icml*, volume 1, pages 609–616. Citeseer, 2001.
- B. Zadrozny and C. Elkan. Transforming classifier scores into accurate multiclass probability estimates. In *Proceedings of the eighth ACM SIGKDD international conference on Knowledge discovery and data mining*, pages 694–699, 2002.

A Code

Code implementing SC-CP and for reproducing our experiments are available upon request and will be made publicly available in a later version of this technical report.

B Additional figures



(a) Avg. interval width with varying calibration error.

Figure 4: Figure 4a shows the marginal coverage corresponding to the interval widths of Figure 2a for varying ℓ^2 -calibration errors in f .

C Proofs

Proof of Theorem 4.1. It can be verified that an *isotonic calibrator class* Θ_{iso} satisfies the following properties: (a) It consists of univariate regression trees (i.e., piecewise constant functions) that are monotonically nondecreasing; (b) For all elements $\theta \in \Theta_{\text{iso}}$ and transformations $g : \mathbb{R} \rightarrow \mathbb{R}$, it holds that $g \circ \theta \in \Theta_{\text{iso}}$. Property (a) holds by definition. Property (b) is satisfied since constraining the maximum number of constant segments by $k(n)$ does not constrain the possible values that the function may take in a given constant region. We note that the result of this theorem holds in general for any function class Θ_{iso} that satisfies (a) and (b).

Recall from Alg. 1 that $f_n^{(X_{n+1}, Y_{n+1})} = \theta_n^{(X_{n+1}, Y_{n+1})} \circ f$, where $\theta_n^{(X_{n+1}, Y_{n+1})} \in \Theta_{\text{iso}}$ is an isotonic calibrator satisfying $f_n^{(X_{n+1}, Y_{n+1})} = \theta_n^{(X_{n+1}, Y_{n+1})} \circ f$. By definition, recall that the isotonic calibrator class Θ_{iso} satisfies

the invariance property that, for all $g : \mathbb{R} \rightarrow \mathbb{R}$, the inclusion $\theta \in \Theta_{iso}$ implies $g \circ \theta \in \Theta_{iso}$. Hence, for all $g : \mathbb{R} \rightarrow \mathbb{R}$ and $\varepsilon > 0$, it also holds that $(1 + \varepsilon g) \circ \theta_n^{(X_{n+1}, Y_{n+1})}$ lies in Θ_{iso} . Now, we use that $(1 + \varepsilon g) \circ \theta_n^{(X_{n+1}, Y_{n+1})} \circ f = (1 + \varepsilon g) \circ f_n^{(X_{n+1}, Y_{n+1})}$ and that $f_n^{(X_{n+1}, Y_{n+1})}$ is an empirical risk minimizer over the class $\{g \circ f : g \in \Theta_{iso}\}$. Using these two observations, the first order derivative equations characterizing the empirical risk minimizer $f_n^{(X_{n+1}, Y_{n+1})}$ imply, for all $g : \mathbb{R} \rightarrow \mathbb{R}$, that

$$\begin{aligned} \frac{1}{n+1} \sum_{i=1}^{n+1} (g \circ f_n^{(X_{n+1}, Y_{n+1})})(X_i) \left\{ Y_i - f_n^{(X_{n+1}, Y_{n+1})}(X_i) \right\} &= \frac{d}{d\varepsilon} \left[\frac{1}{n+1} \sum_{i=1}^{n+1} \left\{ Y_i - (1 + \varepsilon g) \circ f_n^{(X_{n+1}, Y_{n+1})} \right\}^2 \right] \Bigg|_{\varepsilon=0} \\ &= 0. \end{aligned} \quad (4)$$

Taking expectations of both sides of the above display, we conclude

$$\frac{1}{n+1} \sum_{i=1}^{n+1} \mathbb{E} \left[(g \circ f_n^{(X_{n+1}, Y_{n+1})})(X_i) \left\{ Y_i - f_n^{(X_{n+1}, Y_{n+1})}(X_i) \right\} \right] = 0. \quad (5)$$

We now use the fact that $\{(X_i, Y_i, f_n^{(X_{n+1}, Y_{n+1})}(X_i)) : i \in [n+1]\}$ are exchangeable, since $\{(X_i, Y_i)\}_{i=1}^{n+1}$ are exchangeable by **C1** and the function $f_n^{(X_{n+1}, Y_{n+1})}$ is invariant under permutations of $\{(X_i, Y_i)\}_{i=1}^{n+1}$. Consequently, Equation (5) remains true if we replace each $(X_i, Y_i, f_n^{(X_{n+1}, Y_{n+1})}(X_i))$ with $i \in [n]$ by $(X_{n+1}, Y_{n+1}, f_n^{(X_{n+1}, Y_{n+1})}(X_{n+1}))$. That is,

$$\begin{aligned} \mathbb{E} \left[(g \circ f_n^{(X_{n+1}, Y_{n+1})})(X_{n+1}) \left\{ Y_{n+1} - f_n^{(X_{n+1}, Y_{n+1})}(X_{n+1}) \right\} \right] &= \frac{1}{n+1} \sum_{i=1}^{n+1} \mathbb{E} \left[(g \circ f_n^{(X_{n+1}, Y_{n+1})})(X_{n+1}) \left\{ Y_{n+1} - f_n^{(X_{n+1}, Y_{n+1})}(X_{n+1}) \right\} \right] \\ &= \frac{1}{n+1} \sum_{i=1}^{n+1} \mathbb{E} \left[(g \circ f_n^{(X_{n+1}, Y_{n+1})})(X_i) \left\{ Y_i - f_n^{(X_{n+1}, Y_{n+1})}(X_i) \right\} \right] \\ &= 0. \end{aligned}$$

By the law of iterated conditional expectations, the preceding display further implies

$$\mathbb{E} \left[(g \circ f_n^{(X_{n+1}, Y_{n+1})})(X_{n+1}) \left\{ \mathbb{E}[Y_{n+1} | f_n^{(X_{n+1}, Y_{n+1})}(X_{n+1})] - f_n^{(X_{n+1}, Y_{n+1})}(X_{n+1}) \right\} \right] = 0.$$

Taking $g : \mathbb{R} \rightarrow \mathbb{R}$ to be defined by $(g \circ f_n^{(X_{n+1}, Y_{n+1})})(X_{n+1}) := \mathbb{E}[Y_{n+1} | f_n^{(X_{n+1}, Y_{n+1})}(X_{n+1})] - f_n^{(X_{n+1}, Y_{n+1})}(X_{n+1})$, we find

$$\mathbb{E} \left[\left\{ \mathbb{E}[Y_{n+1} | f_n^{(X_{n+1}, Y_{n+1})}(X_{n+1})] - f_n^{(X_{n+1}, Y_{n+1})}(X_{n+1}) \right\}^2 \right] = 0.$$

The above equality implies $\mathbb{E}[Y_{n+1} | f_n^{(X_{n+1}, Y_{n+1})}(X_{n+1})] = f_n^{(X_{n+1}, Y_{n+1})}(X_{n+1})$ almost surely, as desired. \square

Proof of Theorem 4.2. Recall, for a quantile level $\alpha \in (0, 1)$, the “pinball” quantile loss function ℓ_α is given by

$$\ell_\alpha(f(x), s) := \begin{cases} \alpha(s - f(x)) & \text{if } s \geq f(x), \\ (1 - \alpha)(f(x) - s) & \text{if } s < f(x). \end{cases}$$

As established in [Gibbs et al. 2023](#), each subgradient of $\ell_\alpha(\cdot, x)$ at f in the direction g , for some $\beta \in [\alpha - 1, \alpha]$, given by:

$$\partial_{\varepsilon[\beta]} \{ \ell_\alpha(f(x) + \varepsilon g(x), s) \} \Big|_{\varepsilon=0} := \mathbf{1}(f(x) \neq s)g(x)\{\alpha - \mathbf{1}(f < s)\} + \mathbf{1}(f(x) = s)\beta g(x).$$

For $(x, y) \in \mathcal{X} \times \mathcal{Y}$, define the empirical risk minimizer:

$$\rho_n^{(x,y)} \in \operatorname{argmin}_{\theta \circ f_n^{(x,y)}; \theta: \mathbb{R} \rightarrow \mathbb{R}} \sum_{i=1}^n \ell_\alpha \left(\theta \circ f_n^{(x,y)}(X_i), S_i^{(x,y)} \right) + \ell_\alpha \left(\theta \circ f_n^{(x,y)}(x), S_{n+1}^{(x,y)} \right).$$

Then, since the isotonic calibrated predictor $f_n^{(x,y)}$ is piece-wise constant and the above optimization problem is unconstrained in the map $\theta : \mathbb{R} \rightarrow \mathbb{R}$, it holds that the evaluation $\rho_n^{(x,y)}(x)$ lies in the solution set:

$$\operatorname{argmin}_{q \in \mathbb{R}} \sum_{i=1}^n K_i(f_n^{(x,y)}, x) \cdot \ell_\alpha(q, S_i^{(x,y)}) + \ell_\alpha(q, S_{n+1}^{(x,y)}),$$

where $K_i(f_n^{(x,y)}, x) = \mathbf{1}\{f_n^{(x,y)}(X_i) = f_n^{(x,y)}(x)\}$. Consequently, we see that the empirical quantile $\rho_n^{(x,y)}(x)$ defined in [Alg. 2](#) coincides with the evaluation of the empirical risk minimizer $\rho_n^{(x,y)}(\cdot)$ at x , as suggested by our notation.

We will now theoretically analyze [Alg. 2](#) by studying the empirical risk minimizer $x' \mapsto \rho_n^{(X_{n+1}, Y_{n+1})}(x')$. To do so, we modify the arguments used to establish [Theorem 2](#) of [Gibbs et al. 2023](#). As in [Gibbs et al. 2023](#), we begin by examining the first-order equations of the convex optimization problem defining $x' \mapsto \rho_n^{(X_{n+1}, Y_{n+1})}(x')$.

Studying first-order equations of convex problem: Given any transformation $\theta : \mathbb{R} \rightarrow \mathbb{R}$, each subgradient of the map

$$\varepsilon \mapsto \ell_\alpha \left(\rho_n^{(X_{n+1}, Y_{n+1})}(X_i) + \varepsilon \theta \circ f_n^{(X_{n+1}, Y_{n+1})}(X_i), S_i^{(X_{n+1}, Y_{n+1})} \right)$$

is, for some $\beta \in [\alpha - 1, \alpha]^{n+1}$, of the following form:

$$\partial_{\varepsilon[\beta]} \left\{ \ell_\alpha \left(\rho_n^{(X_{n+1}, Y_{n+1})}(X_i) + \varepsilon \theta \circ f_n^{(X_{n+1}, Y_{n+1})}(X_i), S_i^{(X_{n+1}, Y_{n+1})} \right) \right\} \Big|_{\varepsilon=0}$$

$$:= \begin{cases} \theta \circ f_n^{(X_{n+1}, Y_{n+1})}(X_i) \{\alpha - 1(\rho_n^{(X_{n+1}, Y_{n+1})}(X_i) < S_i^{(X_{n+1}, Y_{n+1})})\} & \text{if } S_i^{(X_{n+1}, Y_{n+1})} \neq \rho_n^{(X_{n+1}, Y_{n+1})}(X_i), \\ \beta_i(\theta \circ f_n^{(X_{n+1}, Y_{n+1})})(X_i) & \text{if } S_i^{(X_{n+1}, Y_{n+1})} = \rho_n^{(X_{n+1}, Y_{n+1})}(X_i). \end{cases}$$

Now, since $\rho_n^{(X_{n+1}, Y_{n+1})}$ is an empirical risk minimizer of the quantile loss over the class $\{\theta \circ f_n^{(X_{n+1}, Y_{n+1})}; \theta : \mathbb{R} \rightarrow \mathbb{R}\}$, there exists some vector $\beta^* = (\beta_1^*, \dots, \beta_{n+1}^*) \in [\alpha - 1, \alpha]^{n+1}$ such that

$$0 = \frac{1}{n+1} \sum_{i=1}^{n+1} \mathbb{1}\{S_i^{(X_{n+1}, Y_{n+1})} \neq \rho_n^{(X_{n+1}, Y_{n+1})}(X_i)\} \left[\theta \circ f_n^{(X_{n+1}, Y_{n+1})}(X_i) \{\alpha - 1(\rho_n^{(X_{n+1}, Y_{n+1})}(X_i) < S_i^{(X_{n+1}, Y_{n+1})})\} \right] \\ + \frac{1}{n+1} \sum_{i=1}^{n+1} \mathbb{1}\{S_i^{(X_{n+1}, Y_{n+1})} = \rho_n^{(X_{n+1}, Y_{n+1})}(X_i)\} \left[\beta_i^*(\theta \circ f_n^{(X_{n+1}, Y_{n+1})})(X_i) \right]$$

The above display can be rewritten as:

$$\frac{1}{n+1} \sum_{i=1}^{n+1} \left[\theta \circ f_n^{(X_{n+1}, Y_{n+1})}(X_i) \{\alpha - 1(\rho_n^{(X_{n+1}, Y_{n+1})}(X_i) < S_i^{(X_{n+1}, Y_{n+1})})\} \right] \\ = \frac{1}{n+1} \sum_{i=1}^{n+1} \mathbb{1}\{S_i^{(X_{n+1}, Y_{n+1})} = \rho_n^{(X_{n+1}, Y_{n+1})}(X_i)\} \left[(1 - \beta_i^*)(\theta \circ f_n^{(X_{n+1}, Y_{n+1})})(X_i) \right]. \quad (6)$$

Now, observe that the collection of random variables

$$\left\{ (f_n^{(X_{n+1}, Y_{n+1})}(X_i), S_i^{(X_{n+1}, Y_{n+1})}, \rho_n^{(X_{n+1}, Y_{n+1})}(X_i)) : i \in [n+1] \right\}$$

are exchangeable, since $\{(X_i, Y_i) : i \in [n+1]\}$ are exchangeable by [C1](#) and the functions $f_n^{(X_{n+1}, Y_{n+1})}(\cdot)$ and $\rho_n^{(X_{n+1}, Y_{n+1})}(\cdot)$ are unchanged under permutations of the training data $\{(X_i, Y_i)\}_{i \in [n+1]}$. Thus, the expectation of the left-hand side of Equation (6) can be expressed as:

$$\mathbb{E} \left[\frac{1}{n+1} \sum_{i=1}^{n+1} \left[\theta \circ f_n^{(X_{n+1}, Y_{n+1})}(X_i) \{\alpha - 1(\rho_n^{(X_{n+1}, Y_{n+1})}(X_i) < S_i^{(X_{n+1}, Y_{n+1})})\} \right] \right] \\ = \frac{1}{n+1} \sum_{i=1}^{n+1} \mathbb{E} \left[\theta \circ f_n^{(X_{n+1}, Y_{n+1})}(X_i) \{\alpha - 1(\rho_n^{(X_{n+1}, Y_{n+1})}(X_i) < S_i^{(X_{n+1}, Y_{n+1})})\} \right] \\ = \mathbb{E} \left[\theta \circ f_n^{(X_{n+1}, Y_{n+1})}(X_{n+1}) \{\alpha - 1(\rho_n^{(X_{n+1}, Y_{n+1})}(X_{n+1}) < S_{n+1}^{(X_{n+1}, Y_{n+1})})\} \right],$$

where the final inequality follows from exchangeability. Combining this with Equation (6), we find

$$\mathbb{E} \left[\theta \circ f_n^{(X_{n+1}, Y_{n+1})}(X_{n+1}) \{\alpha - 1(\rho_n^{(X_{n+1}, Y_{n+1})}(X_{n+1}) < S_{n+1}^{(X_{n+1}, Y_{n+1})})\} \right] \quad (7)$$

$$= \mathbb{E} \left[\mathbb{1}\{S_i^{(X_{n+1}, Y_{n+1})} = \rho_n^{(X_{n+1}, Y_{n+1})}(X_i)\} \left[(1 - \beta_i^*)(\theta \circ f_n^{(X_{n+1}, Y_{n+1})})(X_i) \right] \right] \quad (8)$$

Lower bound on coverage: We first obtain the lower coverage bound in the theorem statement. Note, for any nonnegative $\theta : \mathbb{R} \rightarrow \mathbb{R}$, that (8) implies:

$$\mathbb{E} \left[\theta \circ f_n^{(X_{n+1}, Y_{n+1})}(X_{n+1}) \{ \alpha - 1(\rho_n^{(X_{n+1}, Y_{n+1})}(X_{n+1}) < S_{n+1}^{(X_{n+1}, Y_{n+1})}) \} \right] \geq 0.$$

This inequality holds since $(1 - \beta_i^*) \geq 0$ and $(\theta \circ f_n^{(X_{n+1}, Y_{n+1})})(X_i) \geq 0$ almost surely, for each $i \in [n+1]$.

By the law of iterated expectations, we then have

$$\mathbb{E} \left[\theta \circ f_n^{(X_{n+1}, Y_{n+1})}(X_{n+1}) \left\{ \alpha - \mathbb{P} \left(\rho_n^{(X_{n+1}, Y_{n+1})}(X_{n+1}) < S_{n+1}^{(X_{n+1}, Y_{n+1})} \mid f_n^{(X_{n+1}, Y_{n+1})}(X_{n+1}) \right) \right\} \right] \geq 0.$$

Taking $\theta : \mathbb{R} \rightarrow \mathbb{R}$ as a nonnegative map that almost surely satisfies

$$\theta \circ f_n^{(X_{n+1}, Y_{n+1})}(X_{n+1}) = 1 \left\{ \alpha \leq \mathbb{P} \left(\rho_n^{(X_{n+1}, Y_{n+1})}(X_{n+1}) < S_{n+1}^{(X_{n+1}, Y_{n+1})} \mid f_n^{(X_{n+1}, Y_{n+1})}(X_{n+1}) \right) \right\},$$

we find

$$-\mathbb{E} \left[\left\{ \alpha - \mathbb{P} \left(\rho_n^{(X_{n+1}, Y_{n+1})}(X_{n+1}) < S_{n+1}^{(X_{n+1}, Y_{n+1})} \mid f_n^{(X_{n+1}, Y_{n+1})}(X_{n+1}) \right) \right\}_- \right] \geq 0,$$

where the map $t \mapsto \{t\}_- := |t|1(t \leq 0)$ extracts the negative part of its input. Multiplying both sides of the previous inequality by -1 , we obtain

$$0 \leq \mathbb{E} \left[\left\{ \alpha - \mathbb{P} \left(\rho_n^{(X_{n+1}, Y_{n+1})}(X_{n+1}) < S_{n+1}^{(X_{n+1}, Y_{n+1})} \mid f_n^{(X_{n+1}, Y_{n+1})}(X_{n+1}) \right) \right\}_- \right] \leq 0.$$

We conclude that the negative part of $\left\{ \alpha - \mathbb{P} \left(\rho_n^{(X_{n+1}, Y_{n+1})}(X_{n+1}) < S_{n+1}^{(X_{n+1}, Y_{n+1})} \mid f_n^{(X_{n+1}, Y_{n+1})}(X_{n+1}) \right) \right\}$ is almost surely zero. Thus, it must be almost surely true that

$$\alpha \geq \mathbb{P} \left(\rho_n^{(X_{n+1}, Y_{n+1})}(X_{n+1}) < S_{n+1}^{(X_{n+1}, Y_{n+1})} \mid f_n^{(X_{n+1}, Y_{n+1})}(X_{n+1}) \right).$$

Note that the event $Y_{n+1} \in \widehat{C}_n(X_{n+1}) = \{y \in \mathcal{Y} : S_{n+1}^{(X_{n+1}, y)} \leq \rho_n^{(X_{n+1}, y)}(X_{n+1})\}$ occurs if, and only if, $\rho_n^{(X_{n+1}, Y_{n+1})}(X_{n+1}) \geq S_{n+1}^{(X_{n+1}, Y_{n+1})}$. As a result, we obtain the desired lower coverage bound:

$$1 - \alpha \leq \mathbb{P} \left(Y_{n+1} \in \widehat{C}_n(X_{n+1}) \mid f_n^{(X_{n+1}, Y_{n+1})}(X_{n+1}) \right).$$

Deviation bound for the coverage: We now bound the deviation of the coverage of SC-CP from the

lower bound. Note, for any $f : \mathbb{R} \rightarrow \mathbb{R}$, that (8) implies:

$$\begin{aligned} & \mathbb{E} \left[\theta \circ f_n^{(X_{n+1}, Y_{n+1})}(X_{n+1}) \{ \alpha - 1(\rho_n^{(X_{n+1}, Y_{n+1})}(X_{n+1}) < S_{n+1}^{(X_{n+1}, Y_{n+1})}) \} \right] \\ & \leq \left| \mathbb{E} \left[1 \{ S_i^{(X_{n+1}, Y_{n+1})} = \rho_n^{(X_{n+1}, Y_{n+1})}(X_i) \} \left[(1 - \beta_i^*)(\theta \circ f_n^{(X_{n+1}, Y_{n+1})})(X_i) \right] \right] \right|. \end{aligned} \quad (9)$$

Using that $(1 - \beta_i^*) \in [0, 1]$ and exchangeability, we can bound the right-hand side of the above as

$$\begin{aligned} & \left| \mathbb{E} \left[\frac{1}{n+1} \sum_{i=1}^{n+1} 1 \{ S_i^{(X_{n+1}, Y_{n+1})} = \rho_n^{(X_{n+1}, Y_{n+1})}(X_i) \} \left[(1 - \beta_i^*)(\theta \circ f_n^{(X_{n+1}, Y_{n+1})})(X_i) \right] \right] \right| \\ & \leq \frac{1}{n+1} \mathbb{E} \left[\left\{ \max_{i \in [n+1]} |(\theta \circ f_n^{(X_{n+1}, Y_{n+1})})(X_i)| \right\} \sum_{i=1}^{n+1} 1 \{ S_i^{(X_{n+1}, Y_{n+1})} = \rho_n^{(X_{n+1}, Y_{n+1})}(X_i) \} \right]. \end{aligned}$$

Next, since there are no ties by C4, the event $1 \{ S_i^{(X_{n+1}, Y_{n+1})} = \rho_n^{(X_{n+1}, Y_{n+1})}(X_i) \}$ for some index $i \in [n+1]$ can only occur once per piecewise constant segment of $\rho_n^{(X_{n+1}, Y_{n+1})}$, since, otherwise, $S_i^{(X_{n+1}, Y_{n+1})} = \rho_n^{(X_{n+1}, Y_{n+1})}(X_i) = \rho_n^{(X_{n+1}, Y_{n+1})}(X_j) = S_j^{(X_{n+1}, Y_{n+1})}$ for some $i \neq j$. However, $\rho_n^{(X_{n+1}, Y_{n+1})}$ is a transformation of $f_n^{(X_{n+1}, Y_{n+1})}$ and, therefore, has the same number of constant segments as $f_n^{(X_{n+1}, Y_{n+1})}$. In particular, by C3, $\rho_n^{(X_{n+1}, Y_{n+1})}$ has no more than $n^{1/3} \text{polylog}(n)$ constant segments. It therefore holds that

$$\sum_{i=1}^{n+1} 1 \{ S_i^{(X_{n+1}, Y_{n+1})} = \rho_n^{(X_{n+1}, Y_{n+1})}(X_i) \} \leq n^{1/3} \text{polylog}(n).$$

Using that $\frac{n^{1/3} \text{polylog}(n)}{n+1} \leq \frac{\text{polylog}(n)}{n^{2/3}}$, this implies that

$$\frac{1}{n+1} \mathbb{E} \left[\max_{i \in [n+1]} |(\theta \circ f_n^{(X_{n+1}, Y_{n+1})})(X_i)| \sum_{i=1}^{n+1} 1 \{ S_i^{(X_{n+1}, Y_{n+1})} = \rho_n^{(X_{n+1}, Y_{n+1})}(X_i) \} \right] \leq \frac{\text{polylog}(n)}{n^{2/3}} \mathbb{E} \left[\max_{i \in [n+1]} |(\theta \circ f_n^{(X_{n+1}, Y_{n+1})})(X_i)| \right]$$

Combining this bound with (9), we find

$$\mathbb{E} \left[\theta \circ f_n^{(X_{n+1}, Y_{n+1})}(X_{n+1}) \{ \alpha - 1(\rho_n^{(X_{n+1}, Y_{n+1})}(X_{n+1}) < S_{n+1}^{(X_{n+1}, Y_{n+1})}) \} \right] \leq \frac{\text{polylog}(n)}{n^{2/3}} \mathbb{E} \left[\max_{i \in [n+1]} |(\theta \circ f_n^{(X_{n+1}, Y_{n+1})})(X_i)| \right].$$

By the law of iterated expectations, we then have

$$\begin{aligned} & \mathbb{E} \left[\theta \circ f_n^{(X_{n+1}, Y_{n+1})}(X_{n+1}) \left\{ \alpha - \mathbb{P} \left(\rho_n^{(X_{n+1}, Y_{n+1})}(X_{n+1}) < S_{n+1}^{(X_{n+1}, Y_{n+1})} \mid f_n^{(X_{n+1}, Y_{n+1})}(X_{n+1}) \right) \right\} \right] \\ & \leq \frac{\text{polylog}(n)}{n^{2/3}} \mathbb{E} \left[\max_{i \in [n+1]} |(\theta \circ f_n^{(X_{n+1}, Y_{n+1})})(X_i)| \right]. \end{aligned}$$

Next, let $\mathcal{V} \subset \mathbb{R}$ denote the support of the random variable $f_n^{(X_{n+1}, Y_{n+1})}(X_{n+1})$. Then, taking θ to be $t \mapsto 1(t \in \mathcal{V}) \text{sign} \left\{ \alpha - \mathbb{P} \left(\rho_n^{(X_{n+1}, Y_{n+1})}(X_{n+1}) < S_{n+1}^{(X_{n+1}, Y_{n+1})} \mid f_n^{(X_{n+1}, Y_{n+1})}(X_{n+1}) = t \right) \right\}$, which falls almost

surely in $\{-1, 1\}$, we obtain the mean absolute error bound:

$$\mathbb{E} \left| \alpha - \mathbb{P} \left(\rho_n^{(X_{n+1}, Y_{n+1})}(X_{n+1}) < S_{n+1}^{(X_{n+1}, Y_{n+1})} \mid f_n^{(X_{n+1}, Y_{n+1})}(X_{n+1}) \right) \right| \leq \frac{\text{polylog}(n)}{n^{2/3}}.$$

The result then follows noting that the event $Y_{n+1} \notin \widehat{C}_n(X_{n+1}) = \{y \in \mathcal{Y} : S_{n+1}^{(X_{n+1}, y)} \leq \rho_n^{(X_{n+1}, y)}(X_{n+1})\}$ occurs if, and only if, $\rho_n^{(X_{n+1}, Y_{n+1})}(X_{n+1}) < S_{n+1}^{(X_{n+1}, Y_{n+1})}$. □

Proof of Theorem 4.3. Let P_{n+1} denote the empirical distribution of $\{(X_i, Y_i)\}_{i=1}^{n+1}$ and let P_n denote the empirical distribution of $\{(X_i, Y_i)\}_{i=1}^n$. For any function $g : \mathcal{X} \times \mathcal{Y} \rightarrow \mathbb{R}$: we use the following empirical process notation: $Pg := \int g(x, y) dP(x, y)$, $P_{n+1}g := \int g(x, y) dP_{n+1}(x, y)$, and $P_n g := \int g(x, y) dP_n(x, y)$.

Define the risk functions $R_n^{(x, y)}(\theta) := \frac{1}{n+1} \sum_{i=1}^n \{S_\theta(X_i, Y_i)\}^2 + \frac{1}{n+1} \{S_\theta(x, y)\}^2$, $R_{n+1}(\theta) := \frac{1}{n+1} \sum_{i=1}^{n+1} \{S_\theta(X_i, Y_i)\}^2$, and $R_0(\theta) := \int \{S_\theta(x, y)\}^2 dP(x, y)$. Moreover, define the risk minimizers as $\theta_n^{(x, y)} := \operatorname{argmin}_{\theta \in \Theta_{iso}} R_n^{(x, y)}(\theta)$ and $\theta_0 := \operatorname{argmin}_{\theta \in \Theta_{iso}} R_0(\theta)$. Observe that $R_n^{(x, y)}(\theta_n^{(x, y)}) - R_n^{(x, y)}(\theta_0) \leq 0$ since f_n minimizes R_n over Θ_{iso} . Using this inequality, it follows that

$$\begin{aligned} R_0(\theta_n^{(x, y)}) - R_0(\theta_0) &= R_0(\theta_n^{(x, y)}) - R_n^{(x, y)}(\theta_n^{(x, y)}) \\ &\quad + R_n^{(x, y)}(\theta_n^{(x, y)}) - R_n^{(x, y)}(\theta_0) + R_n^{(x, y)}(\theta_0) - R_0(\theta_0) \\ &\leq R_0(\theta_n^{(x, y)}) - R_n^{(x, y)}(\theta_n^{(x, y)}) - \left\{ R_n^{(x, y)}(\theta_0) - R_0(\theta_0) \right\} \\ &\leq R_0(\theta_n^{(x, y)}) - R_{n+1}(\theta_n^{(x, y)}) - \left\{ R_{n+1}(\theta_0) - R_0(\theta_0) \right\} \\ &\quad + R_n^{(x, y)}(\theta_n^{(x, y)}) - R_{n+1}(\theta_n^{(x, y)}) - \left\{ R_n^{(x, y)}(\theta_0) - R_{n+1}(\theta_0) \right\}. \end{aligned}$$

The first term on the right-hand side of the above display can be written as

$$R_0(\theta_n^{(x, y)}) - R_{n+1}(\theta_n^{(x, y)}) - \left\{ R_{n+1}(\theta_0) - R_0(\theta_0) \right\} = (P_{n+1} - P) \left[\{S_{\theta_n^{(x, y)}}\}^2 - \{S_{\theta_0}\}^2 \right].$$

We now bound the second term, $R_n^{(x, y)}(\theta_n^{(x, y)}) - R_{n+1}(\theta_n^{(x, y)}) - \left\{ R_n^{(x, y)}(\theta_0) - R_{n+1}(\theta_0) \right\}$. For any $\theta \in \Theta_{iso}$, observe that

$$R_n^{(x, y)}(\theta) - R_{n+1}(\theta) = \frac{1}{n+1} \left[\{y - \theta \circ f(x)\}^2 - \{Y_{n+1} - \theta \circ f(X_{n+1})\}^2 \right].$$

We know that $\theta_n^{(x, y)}$ and θ_0 , being defined via isotonic regression, are uniformly bounded by $B := \sup_{y \in \mathcal{Y}} |y|$, which is finite by C7. Therefore,

$$\left| R_n^{(x, y)}(\theta_n^{(x, y)}) - R_{n+1}(\theta_n^{(x, y)}) - \left\{ R_n^{(x, y)}(\theta_0) - R_{n+1}(\theta_0) \right\} \right| \leq \frac{8B^2}{n+1} = O(n^{-1}).$$

Combining the previous displays, we obtain the excess risk bound

$$R_0(\theta_n^{(x,y)}) - R_0(\theta_0) \leq (P_{n+1} - P) \left[\{S_{\theta_n^{(x,y)}}\}^2 - \{S_{\theta_0}\}^2 \right] + O(n^{-1}). \quad (10)$$

Next, we claim that $R_0(\theta_n^{(x,y)}) - R_0(\theta_0) \geq \|(\theta_n^{(x,y)} \circ f) - (\theta_0 \circ f)\|_P^2$. To show this, expanding the squares, note, pointwise for each $x \in \mathcal{X}$ and $y \in \mathcal{Y}$, that

$$\begin{aligned} \{S_{\theta_n^{(x,y)}}(x,y)\}^2 - \{S_{\theta_0}(x,y)\}^2 &= \{\theta_n^{(x,y)} \circ f(x)\}^2 - \{\theta_0 \circ f(x)\}^2 - 2y \left\{ (\theta_n^{(x,y)} \circ f)(x) - (\theta_0 \circ f)(x) \right\} \\ &= \left\{ (\theta_n^{(x,y)} \circ f)(x) + (\theta_0 \circ f)(x) - 2y \right\} \left\{ (\theta_n^{(x,y)} \circ f)(x) - (\theta_0 \circ f)(x) \right\}. \end{aligned}$$

Consequently,

$$R_0(\theta_n^{(x,y)}) - R_0(\theta_0) = \int \left\{ (\theta_n^{(x,y)} \circ f)(x) + (\theta_0 \circ f)(x) - 2y \right\} \left\{ (\theta_n^{(x,y)} \circ f)(x) - (\theta_0 \circ f)(x) \right\} dP(x). \quad (11)$$

By [C5](#), Θ_{iso} consists of all isotonic regression trees and is, therefore, a convex space. Thus, the first-order derivative equations defining the population minimizer θ_0 imply that

$$\int \left\{ \theta_n^{(x,y)} \circ f(x) - \theta_0 \circ f(x) \right\} \{y - \theta_0 \circ f(x)\} dP(x,y) \leq 0. \quad (12)$$

Combining [\(11\)](#) and [\(12\)](#), we find

$$\begin{aligned} R_0(\theta_n^{(x,y)}) - R_0(\theta_0) &= \int \left\{ (\theta_n^{(x,y)} \circ f)(x) - (\theta_0 \circ f)(x) \right\}^2 dP(x) \\ &\quad + 2 \int \{(\theta_0 \circ f)(x) - y\} \left\{ (\theta_n^{(x,y)} \circ f)(x) - (\theta_0 \circ f)(x) \right\} dP(x) \\ &\geq \int \left\{ (\theta_n^{(x,y)} \circ f)(x) - (\theta_0 \circ f)(x) \right\}^2 dP(x), \end{aligned}$$

as desired. Combining this lower bound with [\(10\)](#), we obtain the inequality

$$\int \left\{ (\theta_n^{(x,y)} \circ f)(x) - (\theta_0 \circ f)(x) \right\}^2 dP(x) \leq R_0(\theta_n^{(x,y)}) - R_0(\theta_0) \leq (P_n - P) \left[\{S_{\theta_n^{(x,y)}}\}^2 - \{S_{\theta_0}\}^2 \right] + O(1/n) \quad (13)$$

Define $\delta_n := \sqrt{\int \left\{ (\theta_n^{(x,y)} \circ f)(x) - (\theta_0 \circ f)(x) \right\}^2 dP(x)}$, the bound $B := \sup_{y \in \mathcal{Y}} |y|$, and the function class,

$$\Theta_{1,n} := \{(x,y) \mapsto \{(\theta_1 + \theta_2) \circ f - 2y\} \{(\theta_1 - \theta_2) \circ f\}\}.$$

Using this notation, (13) implies

$$\begin{aligned}\delta_n^2 &\leq \sup_{\theta_1, \theta_2 \in \Theta_{iso}: \|\theta_1 - \theta_2\| \leq \delta_n} \int \{(\theta_1 + \theta_2) \circ f(x) - 2y\} \{(\theta_1 - \theta_2) \circ f(x)\} d(P_n - P)(x, y) + O(1/n) \\ &\leq \sup_{h \in \Theta_{1,n}: \|h\| \leq 4B\delta_n} (P_n - P)h + O(1/n)\end{aligned}$$

Using the above inequality and C6, we will use an argument similar to the proof of Theorem 3 in [van der Laan et al. 2023](#) to establish that $\delta_n = O_p(n^{-1/3})$. This rate then implies the result of the theorem. To see this, note, by the reverse triangle inequality,

$$\begin{aligned}\left| S_n^{(x,y)}(y', x') - S_0(x', y') \right| &= \left| |y' - \theta_n^{(x,y)}(x')| - |y' - \theta_0(x')| \right| \\ &\leq \left| \theta_0(x') - \theta_n^{(x,y)}(x') \right|.\end{aligned}$$

Squaring and integrating the left- and right-hand sides, we find

$$\int \left| S_n^{(x,y)}(y', x') - S_0(x', y') \right|^2 dP(x', y') \leq \int \left| \theta_0(x') - \theta_n^{(x,y)}(x') \right|^2 dP(x') = \delta_n^2,$$

as desired.

We now establish that $\delta_n = O_p(n^{-1/3})$. For a function class \mathcal{F} , let $N(\epsilon, \mathcal{F}, L_2(P))$ denote the ϵ -covering number ([van der Vaart and Wellner, 1996](#)) of \mathcal{F} and define the uniform entropy integral of \mathcal{F} by

$$\mathcal{J}(\delta, \mathcal{F}) := \int_0^\delta \sup_Q \sqrt{\log N(\epsilon, \mathcal{F}, L_2(Q))} d\epsilon,$$

where the supremum is taken over all discrete probability distributions Q . We note that

$$\mathcal{J}(\delta, \Theta_{1,n}) = \int_0^\delta \sup_Q \sqrt{N(\epsilon, \Theta_{1,n}, \|\cdot\|_Q)} d\epsilon = \int_0^\delta \sup_Q \sqrt{N(\epsilon, \Theta_{iso}, \|\cdot\|_{Q \circ f^{-1}})} d\epsilon = \mathcal{J}(\delta, \Theta_{iso}),$$

where $Q \circ f^{-1}$ is the push-forward probability measure for the random variable $f(W)$. Additionally, the covering number bound for bounded monotone functions given in Theorem 2.7.5 of [van der Vaart and Wellner 1996](#) implies that

$$\mathcal{J}(\delta, \Theta_{1,n}) = \mathcal{J}(\delta, \Theta_{iso}) \lesssim \sqrt{\delta}.$$

Recall that f is obtained from an external dataset, say \mathcal{E}_n , independent of the calibration data. Noting that f is deterministic conditional on a training dataset \mathcal{E}_n . Applying Theorem 2.1 of [Van Der Vaart and Wellner](#)

2011 conditional on \mathcal{E}_n , we obtain, for any $\delta > 0$, that

$$\begin{aligned} E \left[\sup_{h \in \Theta_{1,n}: \|h\| \leq 4B\delta} (P_n - P)h \mid \mathcal{E}_n \right] &\lesssim n^{-1/2} \mathcal{J}(\delta, \Theta_{1,n}) \left(1 + \frac{\mathcal{J}(\delta, \Theta_{1,n})}{\sqrt{n\delta^2}} \right). \\ &\lesssim n^{-1/2} \mathcal{J}(\delta, \Theta_{iso}) \left(1 + \frac{\mathcal{J}(\delta, \Theta_{iso})}{\sqrt{n\delta^2}} \right). \end{aligned}$$

Noting that the right-hand side of the above bound is deterministic, we conclude that

$$E \left[\sup_{h \in \Theta_{1,n}: \|h\| \leq 4B\delta} (P_n - P)h \right] \lesssim n^{-1/2} \mathcal{J}(\delta, \Theta_{iso}) \left(1 + \frac{\mathcal{J}(\delta, \Theta_{iso})}{\sqrt{n\delta^2}} \right).$$

We use the so-called ‘‘peeling’’ argument (van der Vaart and Wellner, 1996) to obtain our bound for δ_n .

Note

$$\begin{aligned} P \left(\delta_n^2 \geq n^{-2/3} 2^M \right) &= \sum_{m=M}^{\infty} P \left(2^{m+1} \geq n^{2/3} \delta_n^2 \geq 2^m \right) \\ &= \sum_{m=M}^{\infty} P \left(2^{m+1} \geq n^{2/3} \delta_n^2 \geq 2^m, \delta_n^2 \leq \sup_{h \in \Theta_{1,n}: \|h\| \leq 4B\delta_n} (P_n - P)h + O(1/n) \right) \\ &= \sum_{m=M}^{\infty} P \left(2^{m+1} \geq n^{2/3} \delta_n^2 \geq 2^m, 2^{2m} n^{-2/3} \leq \sup_{h \in \Theta_{1,n}: \|h\| \leq 4B2^{m+1} n^{-1/3}} (P_n - P)h + O(1/n) \right) \\ &\leq \sum_{m=M}^{\infty} P \left(2^{2m} n^{-2/3} \leq \sup_{h \in \Theta_{1,n}: \|h\| \leq 4B2^{m+1} n^{-1/3}} (P_n - P)h + O(1/n) \right) \\ &\leq \sum_{m=M}^{\infty} \frac{E \left[\sup_{h \in \Theta_{1,n}: \|h\| \leq 4B2^{m+1} n^{-1/3}} (P_n - P)h \right] + O(1/n)}{2^{2m} n^{-2/3}} \\ &\leq \sum_{m=M}^{\infty} \frac{\mathcal{J}(2^{m+1} n^{-1/3}, \Theta_{iso}) \left(1 + \frac{\mathcal{J}(2^{2m+2} n^{-2/3}, \Theta_{iso})}{\sqrt{n} 2^{m+1} n^{-1/3}} \right)}{\sqrt{n} 2^{2m} n^{-2/3}} + \sum_{m=M}^{\infty} \frac{O(1/n)}{2^{2m} n^{-2/3}} \\ &\leq \sum_{m=M}^{\infty} \frac{2^{(m+1)/2} n^{-1/6}}{2^{2m} n^{-1/6}} + \sum_{m=M}^{\infty} \frac{o(1)}{2^{2m}} \\ &\lesssim \sum_{m=M}^{\infty} \frac{2^{(m+1)/2}}{2^{2m}}. \end{aligned}$$

Since $\sum_{m=1}^{\infty} \frac{2^{(m+1)/2}}{2^{2m}} < \infty$, we have that $\sum_{m=M}^{\infty} \frac{2^{(m+1)/2}}{2^{2m}} \rightarrow 0$ as $M \rightarrow \infty$. Therefore, for all $\varepsilon > 0$, we can choose $M > 0$ large enough so that

$$P \left(\delta_n^2 \geq n^{-2/3} 2^M \right) \leq \varepsilon.$$

We conclude that $\delta_n = O_p(n^{-1/3})$ as desired. □